Sex-specific differences in the regulation and function of cellular immunity in *Drosophila*.

Alexandra Dvoskin[1], Celena Cherlan[1], Guy Tanentzapf 1*

1: Department of Cellular and Physiological Sciences, University of British Columbia, Vancouver, Canada.

* Correspondence: tanentz@mail.ubc.ca

Summary

Sex-specific differences in tissue growth and metabolism are prevalent in animals. It is also known that the immune response in humans differs between sexes and results in differential susceptibility of males and females to autoimmune diseases, malignancies, and infectious diseases. However, the mechanisms that mediate these sex-based differences in immunity are not well understood. Here, using the *Drosophila* hematopoietic organ, the lymph gland, which is the production site for immune cells in larva, we show that *Drosophila* exhibit sex-based differences in cellular immunity and investigate the mechanisms that underlie these differences. We found that compared to females, males exhibit smaller lymph glands, have less blood progenitors, and produce less immune cells. By manipulating sex in a tissue-specific manner we show that these sex specific differences are controlled by organ-specific mechanisms involving blood progenitors and their hematopoietic niche. Importantly, we find a sex-specific differential response to insulin signaling, an important regulator of the immune response in the

niche. Finally, we provide evidence for differences in the cellular immune response following infection between males and females. Overall, our results provide mechanistic insight into how sex-differences in immunity are established.

Introduction

Sex differences are common in nature, with many species exhibiting distinct sex-based differences that reflect variations in reproductive strategies, ecological roles, and physiological demands (1,2). In many animals, males and females diverge in terms of overall body size, muscle mass, fat storage, and reproductive tissue development (3,4,5). These differences often arise early in development, persist throughout life, and manifest at multiple levels, from the individual cell, to tissues, organs, and entire organisms. Sex differences are genetically encoded and typically involve hormonal signals that control animal development and homeostasis (6). *Drosophila* has proven to be a powerful model for exploring the genetic underpinning and signaling mechanisms that underlie sex differences (7-10). In flies, sex differences arise early, appearing during embryogenesis, and are pronounced in the adults. Fruit fly males are typically smaller than females, and exhibit marked differences from females in appearance, behavior, and physiology.

It is well established, both in epidemiological and experimental studies, that there are extensive sex differences in immunity in humans (11,12). This has important implications in health and disease, as evidenced, for example, by sex differences in the ability to fight certain infections, respond to vaccines, or by the higher prevalence of

multiple autoimmune conditions in females. It is speculated that sex differences in immunity are attributed to either genetic or hormonal factors and several mechanistic differences in immunity have been uncovered. On a cellular level, innate detection of pathogens is known to differ between males and females, as sex differences have been found in the induction of toll-like receptors (TLR) and the antiviral type I interferon (IFN) response (13,14). Moreover, In both humans and rats, females show a higher activity of monocytes, macrophages and dendritic cells (15,16). Females also tend to mount a more robust adaptive immune response than males by having a higher proportion of active T cells during certain viral infections (17), as well as increased expression, associated with estrogen response elements in their promoter regions, of antiviral and inflammatory genes (18).

Although immunology studies in humans have increasingly included sex as a variable, this has not been the case in *Drosophila*, an important genetic model system for immunity. A recent literature survey found that out of over 1000 papers about the adult immune system in *Drosophila,* almost half did not report sex and only 13% reported results for both males and females separately (19). In the small number of published immunology studies in *Drosophila* that took sex into account, it has been found that there were differences in immune response and survival following infection, with outcomes being pathogen specific. Specifically, viral infections have been found to show a higher rate of mortality in males than females, with surviving females exhibiting increased infertility (20). Bacterial infection studies have shown a complex picture, with sex differences in survival rates following infection with some but not all strains of

bacteria, regardless of whether the bacterial strain in question was gram negative or gram positive (21-25). For example, females were shown to be more susceptible to infection of *Enterococcus faecalis* but less to *S. aureus* or to *Lactococcus lactis*, all of which are gram positive bacteria (19,23,24). Accounting for some of this variation it has been shown that there are sex-specific differences in the regulation of both the IMD and Toll pathways between males and females following infection (22,23). In terms of the cellular immune response, it has been shown that hemocytes may exhibit sex differences in function. This observation was due to the role that the Jun N-terminal kinase (JNK) pathway was found to play in regulating the decision between cell repair and cell death in fly immune cells (26). As a result of sex differences it was found that JNK helps promote tissue maintenance, but only in males, with a loss of function mutation showing higher tissue damage in males post UV radiation (27).

Work in *Drosophila* on hematopoiesis and immunity has focused extensively on the lymph gland, an organ that is responsible for the cellular immune response during larval stages. The primary lobe of the lymph gland is the main site of hematopoiesis in *Drosophila* larval stages and is typically described as being made up of 3 distinct zones: the Posterior Signaling Center (PSC) is a group of a few dozen cells that are thought to have a stem cell niche-like function, the medullary zone houses blood progenitors, and the cortical zone holds differentiated blood cells. Multiple signaling pathways act in the lymph gland to regulate hematopoiesis including the Wingless, Hedgehog, JAK/STAT, BMP and Notch pathways (28-33). Mutations that perturb these signaling pathways result in a variety of defects in lymph gland homeostasis, ranging from depletion of the

progenitor population, overproduction of various mature blood cell lineages, and expansion of the PSC (28,29,31,32,34). Another major signaling pathway known to act in the lymph gland is the insulin/insulin-like growth factor signaling pathway (IIS) (35,36,37). In the lymph gland, the IIS pathway has been shown to regulate both the maintenance and differentiation of blood progenitors as well as maintenance of the PSC (38,39). Moreover, at least two *Drosophila* insulin-like peptides (dILPs), dILP-2 that is secreted by neurons, and dILP-6, that is secreted from the fat body, are known to act in the lymph gland to control hematopoiesis (40,41,42)

.

Here we analyzed sex specific differences in the *Drosophila* lymph gland under homeostatic conditions as well as following bacterial infection. We identified and quantified sex differences in overall cell number as well as in the specific population size of different cell types in the lymph gland. We investigated the mechanisms that mediate these sex differences, identified the source of the relevant regulatory signals as well as explored the role of Insulin signaling in this process. Finally, we explored whether and how sex differences extend to the cellular immune response following infection.

Materials and Methods

2.1 Fly stocks and genetics

All *Drosophila* crosses were kept at 25□ and sustained in vials containing a standard cornmeal fly food (recipe from Bloomington *Drosophila* Stock Center). All lymph gland progenitors were labelled using fluorescent markers *tep4-gal4; UAS-GFP or*

domeMESO GFP. Wildtype larvae in Figure 1 are categorized as w^{1118} flies crossed to *tep4-gal4; UAS GFP*. Wildtype larvae in Figures 8-9 are categorized as CantonS flies crossed to *domeMESO GFP*.

Using the Gal4 system, various tissues were feminized. The drivers used were *elav-gal4* (CNS), *R4-gal4* (fat body), *tep4-gal4* (lymph gland progenitors), and *collier-gal4* (PSC cells). These drivers were crossed to *domeMESO GFP* for controls, and *UAS TraF/CyoGFP ;domeMESO GFP/TM6* for feminization experiments. A UAS control was also used by crossing *UAS TraF/CyoGFP; domeMESO GFP/TM6* to *domeMESO GFP*. To constitutively activate or knockdown insulin receptors in the lymph gland, *Ca-InR* (RRID: BDSC_8250) and *InR RNAi* (RRID: BDSC_51518) were crossed to *domeMESO GFP* as a control and crossed to PSC cell driver *collier=gal4*.

2.2 Larval lymph gland dissections

Wandering third instar larval lymph glands were dissected in ice-cold 1X Phosphate Buffer Saline (PBS) and then fixed in 4% paraformaldehyde (PFA) for 15 minutes. Samples were then washed in 0.1% PTX (1X PBS with 0.1% Triton X [Thermofisher Scientific, BP 151100]) twice for 5 minutes each, then blocked with 16% Neat Goat Serum (NGS) (ab7481, abcam) for 15 minutes, before being incubated in a primary antibody overnight at 4□. The following day, samples were washed again twice in 0.1% PTX for 5 minutes each, blocked in 16% NGS for 15 minutes, before being incubated in a secondary antibody for two hours at room temperature. Samples were washed three times in 0.1% PTX for 5 minutes each, and mounted in VECTASHIELD (Vector Laboratories, H-1000, RRID: AB_2336789) with TOPRO3 iodide (ThermoFisher

Scientific, T3605; 1:500) in glass bottom mounting dishes (MatTek Corporation, 35 mm, P35G-0-14-C).

2.3 Immunohistochemistry

The following primary antibodies were used and diluted in 0.1% PTX: mouse anti-hindsight (1:50, DSHB 1G9, RRID: AB_2617420), mouse anti Antennapedia (1:25, DSHB 4C3, RRID: AB_528082). The following primaries were used and diluted in 0.1% Tween 20 (1X PBS with 0.1% Tween 20 [Fisher BioReagents, BP337-500]): mouse anti- P1 (1:100) (anti-Nim C, a kind gift from Dr. Istvan Ando, Hungarian Academy of Sciences, Hungary).

The following secondary antibody was used, and diluted in 0.1% PTX (for Hnt and Anti staining) or 0.1% Tween 20 (for P1 staining): donkey anti-mouse Cy3 (1:400, Jackson Immunoresearch Laboratories, Code: 715-165-150, RRID: AB_2340813). A 1µl addition of ToPro was added to the secondary antibody dilution.

2.4 Infection

E.coli (a kind gift from Dr. Bret Finlay, The University of British Columbia, Vancouver, Canada) and ECC15 (a kind gift from Dr. Edan Foley, University of Alberta, Edmonton, Canada) were incubated at 37□ and 30□ respectively overnight. Second instar larvae were picked out of food, washed in ddH2O and 70% ethanol, then starved on an agar pad for 2 hours before being placed into 4g of fly food with either 200µl of PBS (control) or 200µL of E.coli or ECC15 resuspended in PBS. Vials were then placed back in 25□ for 9 hours and dissected using protocol described previously.

2.5 Imaging and data analysis

All images were acquired on an Olympus FV1000 inverted confocal microscope, using a 40x lens. Image analysis was done using Olympus Fluoview (Ver.1.7c) and Matlab scripts previously used in Khadiklar, 2017 (68). Total number of nuclei, prohemocytes and plasmatocytes were determined using this Matlab script. Crystal cells and niche cells were counted manually using the cell counter plugin in Image J.

To correct for body size, average weight was taken for males and females of a genotype by collecting 10-12 third instar larvae, weighing them, and dividing total weight by number of larvae weighed. This weight, in milligrams, was then used to correct data points for body size.

Statistics were performed using GraphPad Prism. P values were determined using a two-tailed unpaired t-test, a one way ANOVA with multiple comparisons (Tukey's test), or a two-way ANOVA multiple comparison (Tukey's Test). **** indicates $P<0.0001$, *** indicates $P<0.001$, ** indicates $P<0.01$, * indicates $P<0.05$, ns (non-significant) indicates $P>0.05$. The sample size and statistical method of each analysis were indicated in the figure legends.

Figures 2-7 used a two-way ANOVA (Tukey's test) to determine both p values both in multiple comparisons, as well as an overall genotype:sex interaction value. The multiple comparison significance are shown within the figure, with the exact p values shown in the figure legends as well as the genotype:sex interaction value. While the multiple comparison results can show specific changes and differences between each of the experimental and control groups, the overall interaction constant is a direct test of the

null hypothesis of whether there is a difference between each of the rows (genotypes) that are the same across columns (sex). In this instance, the null hypothesis is that the differences between the genotypes are consistent for males and females. A statistically significant p value would tell us to reject the null hypothesis and that there are differences between the genotypes across the two sexes.

Results

Lymph Glands Exhibit Sex differences

To investigate whether there were sex differences between lymph glands from male and female larva we analysed their organ size in late 3rd instar larva by staining nuclei with DAPI and counting cells using custom image analysis software (see methods). We found that lymph glands from male larvae contained an average of 1587±404 cells (n=59), while lymph glands from females contained on average 2183±501 (n=63), a difference of ~37% in cell number (Fig. 1F). Next, we determined the number of cells in the Posterior Signaling Centre (PSC), the stem cell niche of the lymph gland by staining with an antibody for the Antennapedia (Antp) and performing cell counts (see methods). These counts showed that lymph glands from male larvae contained an average of 68±22 PSC cells (n=59), while lymph glands from female larvae contained on average 91±24 PSC cells (n=63), a difference of ~33% in size (Fig. 1G). To determine the number of progenitors in lymph gland they were labelled with dome-MESO-GFP (42). Automated cell counts showed that lymph glands from male larvae contained an average of 636±190 progenitors (n=59), while lymph glands from female larvae contained on average 830±282 progenitors (n=63), a difference of ~33% in size (Fig.

1H). To determine the number of mature differentiated plasmatocytes and crystal cells we stained lymph gland with P1 and Hindsight (Hnt) specific antibodies followed by automated whole lymph gland cell counts (see methods). These cell counts showed that in lymph glands from male larvae there were on average 22±17 (m=20) and 335±134 (n=22), crystal cells and plasmatocytes, respectively. In comparison in lymph glands from female larvae there were on average of 46±18 (m=28) and 409±172 (n=29), crystal cells and plasmatocytes, respectively, a difference of ~210% in crystal cell numbers and ~22% in plasmatocyte numbers (Fig. 1I-J).

Since it is known that in *Drosophila* males are smaller in size than females we asked if the sex differences we observed between lymph glands from male and female larvae were consistent with the overall size differences between males and females. To this end we corrected, by adjusting for average larvae size, the cell counts obtained from male and female lymph glands, both for overall cell number, as well as for the PSC, progenitors, crystal cells, and plasmatocyte cell counts (see methods, Fig 1F'-J'). This analysis showed that such a correction eliminated differences in the average number of cells in either the entire lymph gland, the PSC, blood progenitors, or plasmatocytes but not for crystal cell number. Taken together our data shows striking sex differences in both the overall size as well as the size of specific cell populations in the larval lymph gland. Moreover, these sex differences appear in line with general, whole animal, sex-based differences in body size, with the exception of the crystal cells, which show a uniquely large population size increase in females, that exceeds what would be expected based on overall trends in body size.

Sex differences in the lymph gland are not mediated by the CNS

Sex differences between tissues can arise due sex-specific behavior of individual cells, that is cell-autonomously, and/or due to sex-specific differences in systemic cues that regulate cell behaviour, that is non cell-autonomously. For example, it has been shown that systemic signals that arise in either the fat body or the central nervous system (CNS) induce differences in cell growth and metabolism in many tissues and organs in the fly (40,41,42). To test whether sex differences in the lymph gland were due to systemic signal originating from the CNS or fat body, we employed a strategy where we feminised these tissues in an otherwise genetically male fly and studied how this impacted overall size as well the size of individual cell populations in the lymph gland. To induce tissue specific feminization we employed the widely used tool of expressing Tra^F in male tissues (44-52). To control for differences in the lymph gland due to variation in genetic background, in addition to the experimental group of flies having both the Gal4 and Tra^F transgene (Gal4/Tra^F), we analysed flies heterozygous for the Tra^F construct (Tra^F/+) and flies heterozygous for the Gal4 driver (Gal4/+). We then compared males and females from each of the two control groups as well as the experimental group. This meant we were comparing 6 different genotypes to each other, which required us to use a two-way ANOVA, Tukey's test (see methods) to determine if any differences we observed were statistically significant. This test not only allows us to compare the significance of changes between groups but provides an “interaction constant” to show whether the experiment supports the existence of sex differences between males and females under the experimental treatment.

When we used the Tra^F construct to feminise the CNS, we observed no significant impact of genetic background on overall lymph gland size, as males and females of both Tra^F and elav-Gal4 control flies had a similar number of cells in their lymph gland compared to each other or the experimental group (Figure 2A-B). Moreover, using these controls showed that CNS feminization had no significant impact on lymph gland size. This meant that the measured interaction constant derived from the two-way ANOVA (Table 1), suggested that sex differences in the total number of cells in male and female lymph glands were not altered by feminization of the CNS. Similarly, despite noting differences in the number of crystal cells per lymph gland in some experimental groups compared to controls, statistical analysis did not support the conclusion that sex differences in the crystal cell number in male and female lymph glands were impacted by feminization of the CNS (Figure 2E-F; Table 1).

Although, in general, the mean number of progenitors in lymph glands was similar between controls and the experimental group, Tra^F expression in females did seem to cause an increase in progenitor numbers (Figure 2I). Nonetheless, sex specific differences in progenitor numbers remained in CNS-feminised males(Figure 2J). This was confirmed by measuring the interaction constant derived from the two-way ANOVA, which showed that sex differences in progenitor numbers in male and female lymph glands were not eliminated by feminization of the CNS (Table 1). Taken as a whole, our data and statistical analysis supported the interpretation that sex differences in the lymph gland are not mediated by the CNS.

Sex differences in the lymph gland are not mediated by the Fat Body

Since systemic signals that arise in the fat body can also induce differences in cell growth and metabolism in the fly (53,54) we asked whether it was involved in mediating sex-differences in the lymph gland. To this end, we feminised the fat body in genetically male flies using the TraF transgene and studied how this impacted overall size as well the size of individual cell populations in the lymph gland. As we did for the CNS feminization experiments, we compared experimental groups of flies having both the R4-Gal4 and Tra^F transgene (R4-Gal4/Tra^F) to controls flies heterozygous for either the Tra^F construct (Tra^F/+) or the Gal4 driver (R4-Gal4/+). We then compared the 6 different genotypes to each other using a two-way ANOVA interaction constant (see methods).

Our control experiments showed that in the genetic background of R4-Gal4, the driver we employed for expression in the fat body, the overall size of the lymph gland was smaller than other backgrounds (Figure 3A). However, since this effect was seen in both males and females it did not impact our interpretation, as we found that feminization of the fat body had no significant impact on size differences between males and female lymph glands (Figure 3A-B, table 1). Analysis of crystal cell numbers showed a higher amount in lymph glands of the experimental group compared to Tra^F and R4-Gal4 controls for both males and females. Despite this increase, we found no significant impact on sex differences in crystal cell numbers upon fat body feminization, as the increase was in both males and females, with a significant difference still present between males and females after feminisation (Figure 3E-F, Table 1). When

progenitor's numbers were analysed we observed a statistically significant increase in their number in the background of the Tra^F transgene (Figure 3I). This complicates the interpretation of this result, and although in terms of absolute numbers of sex differences in progenitor numbers remained, according to the interaction constant derived from the two-way ANOVA, fat body feminization did impact these differences to a certain extent. Taken as a whole, our data and statistical analysis supported the interpretation that sex differences in overall size and crystal cell numbers are not mediated by the fat body. However, we could not conclusively reject the possibility that the fat body contributed to sex differences in progenitor numbers.

Some Sex differences in the lymph gland are mediated by progenitors

Since we did not uncover strong evidence for a role of systemic signals from the CNS or the fat body in mediating sex differences in the lymph gland we shifted our focus to cell autonomous mechanisms. We asked whether the identity of the blood progenitors themselves controlled sex differences. To test this hypothesis, we feminised the blood progenitors in genetically male flies using the Tra^F transgene and studied how this impacted overall size as well the size of individual cell populations in the lymph gland. We again compared experimental group flies to flies heterozygous for either the Tra^F construct (Tra^F/+) or the Gal4 driver (*tep4*-Gal4/+). We then compared the 6 different genotypes to each other and used a two-way ANOVA, Tukey's test, to derive an interaction constant (see methods).

We found that feminization of the progenitors led to an inconclusive effect on sex differences in the size of the lymph gland. Specifically, while sex differences in the number of nuclei between lymph glands of the experimental female and progenitor-feminized males were reduced (Figure 4B), there were no significant differences between the experimental group and controls within each sex (Figure 4A, Table 1). Analysis of crystal cell numbers following progenitor feminization in males showed similar trends (Figure 4E-F), which would suggest no impact on sex differences, however, in this case the interaction constant did support this conclusion, as the interaction constant was not significant (Table 1). This is likely because the number of cells in the lymph gland was in the thousands while the number of crystal cells is in the dozens which makes it more difficult to reach statistical significance. In contrast, analysis of progenitor numbers provided strong evidence for cell autonomous regulation of sex differences. Specifically, when progenitors were feminized in males this was sufficient to eliminate sex differences in progenitor numbers (Figure 4I-J), a conclusion supported by analysing the interaction constant (Table 1). This was despite the observation that in the tep4-Gal4 driver background there were lower progenitor counts compared to other backgrounds. Taken as a whole, our data and statistical analysis was inconclusive in regard to the role of progenitors in mediating sex differences in overall lymph gland size, and did not support a role for progenitors in mediating sex differences in the number of crystal cells. However, we did find a significant role for progenitors in mediating sex differences in progenitor numbers.

Some Sex differences in the lymph gland are mediated by the PSC

The PSC has an established role in orchestrating the behaviour of different cell types in the lymph gland and is therefore a candidate for mediating sex differences. Intriguingly, feminization of the PSC in males, using collier-Gal4, induced an increase in the number of cells in the lymph gland which led, for the most part, to the elimination of sex differences in size between females and PSC-feminized males (Figure 5A-B, Table 1). A similar effect was seen on crystal cell numbers, which were higher in PSC-feminized males and resembled control females (Figure 5E-F, Table 1). The determination of the interaction constant further supported the interpretation that both for overall size and crystal cell number feminization of the PSC had severely curtailed sex differences (Table 1).

Analysis of progenitor numbers following PSC-feminization revealed a more complex picture. In contrast to overall size or crystal cell numbers, there was no significant increase in progenitor numbers in PSC-feminized lymph glands (Figure 5I, Table 1). While sex differences in progenitor numbers were reduced between experimental group males and females by PSC-feminization, analysis of the interaction constant did not provide conclusive support for such a role (Table 1). Nonetheless, our data and statistical analysis did support the interpretation that sex differences in overall lymph gland size and crystal cell numbers were mediated, at least in part, by the PSC.

Sex differences in crystal cell number are mediated by insulin signalling in the PSC.

Insulin signalling is known to be an important mediator of sex differences in size and tissue growth (55-58). Insulin signaling is also known to be active in the PSC in lymph gland to regulate hematopoiesis (41,42). Based on these observations we hypothesized that Insulin signalling, in the PSC, was important in mediating sex differences in the lymph gland. For these experiments we used collier-Gal4 to express either an RNAi to knock down the insulin receptor (InR-RNAi, Figure 6) or a constitutively active version of the Insulin receptor (Ca-InR, Figure 7).

We found that PSC-specific expression of InR-RNAi led to an increase in the number of cells in male lymph glands, but not female lymph glands and that this was sufficient to impact sex differences in size between females and males of the experimental group (Figure 6A-B). However, analysis of the interaction constant for this dataset did not support the interpretation that InR knockdown in the PSC altered sex differences in a statistically significant manner (Table 2). In comparison, crystal cells numbers exhibited a more dramatic effect, as their number was greater in experimental group males in which InR was knocked down in the PSC than in females of comparable genotype (Figure 6E-F). Analysis of the interaction constant test supported the interpretation that InR receptor knockdown in the male PSC had severely curtailed sex differences in crystal cell number (Table 2). Analysis of progenitor numbers following InR knockdown in the PSC was complicated by genetic background effects in the InR-RNAi line. However, we did not observe statistically significant support for changes in sex differences in progenitor numbers following InR knockdown in the PSC in males (Figure 6I-J; Table 2).

Analysis of PSC-specific Insulin pathway activation via expression of Ca-InR revealed a similar picture. PSC-specific expression of Ca-InR did not greatly alter the number of cells in either male or female lymph glands and consequently there was no statistically significant impact on sex differences in organ size between females and males (Figure 7A-B, Table 2). In contrast, crystal cell numbers were impacted by PSC specific activation of insulin signaling in females, which resulted in a statistically significant impact leading to an elimination of sex differences (Figure 7E-F, Table 2). Similar to overall lymph gland size, progenitor numbers were not impacted by PSC specific insulin pathway activation in either males or females and consequently there did not appear to be a significant reduction in sex differences (Figure 7I-J, Table 2).

Based on the two sets of experiments, utilising downregulation or activation of the insulin receptor in the PSC we do not find conclusive support for a function of the Insulin pathway in the PSC in mediating sex differences in overall lymph gland size or progenitor numbers. However, there is robust statistical support for the finding that sex differences in crystal cell number are maintained by tightly controlling the level of signaling of the insulin pathway in the PSC.

Sex-differences are observed in the cellular immune response following infection

Previous studies in adult flies identified sex-specific differences in the immune response in response to infection that led to variation in survival rates. Intriguingly, these differences appeared to be vary substantially based on the strain of bacteria used for

infection (23). We analysed the immune response in males and females of wildtype (Canton-S) exposed to two different strains of bacteria that are known to activate the immune response in flies, *E. coli* and *Pectobacterium carotovorum* (previously known as *Erwinia carotovora carotovora*, or *Ecc15)* (59,58) (see methods). These strains were chosen since in adult flies, they have been shown to act in a sex-specific manner to control behaviour (23,59,61). Infection by feeding with *E.coli* showed a sex-specific increase in organ size and crystal cell count in females, but not in males(Figure 8A,D). Neither sex showed an increase in progenitor count (Figure 8G), and both sexes showed an increase in plasmatocyte count upon infection (Figure 8J). Infection with *P. carotovorum* resulted in significant increase in crystal cell numbers in females but not in males (Figure 9D). In contrast, overall organ size, progenitor numbers, and plasmatocyte numbers were not significantly impacted by infection in either males or females (Figure 9 A,G,J). Taken together these data show that crystal cells production following infection was differentially regulated between male and female fly larvae. Moreover, we observed bacterial strain specific variation in sex-differences.

Discussion

Our work establishes the *Drosophila* larva as a model for analysing sex-based differences in cellular immunity. In this regard we build upon an increasing body of evidence in *Drosophila* that multiple aspects of innate immunity in adults exhibit striking variation between males and females (21-25,61-62). We find that sex impacts various cell types in the lymph gland to different extents under both homeostatic or infection

conditions, and that there are mechanistic differences in how sex differences are established in the various cell types. This supports a more nuanced and complex role for sex in regulating hematopoiesis beyond a simple generalised increased tissue size and cell number (58,64). We found that the PSC, and more specifically insulin signaling from the PSC, mediated certain sex differences but there are other mechanisms in place since we were not able to mechanistically account for all the variance between males and females. Finally, in line with previous findings of sex-differences in the ability to survive infection (21-25) we find sex-differences in the cellular immune response elicited by bacterial infection. Moreover, and consistent with previous findings (21-25), sex differences in the cellular immune response differed depending on the bacterial strain used for infection, indicating a complex relationship between sex, immunity, and infection. Taken together our work not only functions as an initial characterization of baseline sex-differences in fly hematopoiesis and in cellular immunity but also identifies important areas for future exploration.

Although the existence of sex-differences in innate immunity in fly adults is well established (21,23), it is not yet standard practice to consider sex as a variable in studies that focus on the larval lymph gland. Based on our findings, we believe there is a substantial argument that in the future it should become a standard practice, for all phenotypic characterization of the lymph gland, to consider sex as a key variable. This will mean initially separating dissected larvae and separately recording and analysing data from male and female larvae. We would argue that it should also become the standard, whatever the genotype being analysed, to report data for both sexes.

Although some aspects of larval immunity may not vary greatly between males and females under normal conditions, for example we did not detect a great deal of sex differences in plasmatocyte numbers, these differences might become apparent under specific experimental conditions. Our study did not aim to serve as an exhaustive compendium of all sex based differences in the lymph gland, we suspect these vary considerably based on the genetic background and experimental conditions. Rather our aim was to establish that sex-differences are pervasive in the lymph gland and to provide some insight into the mechanisms that are responsible for these differences. We predict that as more researchers in the field separately report data for males and females for various lymph gland phenotypes the number of documented sex differences will greatly expand.

Our analysis argues for an important role for the *Drosophila* lymph gland niche, the PSC, in at least a subset of sex differences. For the phenotypes we assessed we did not find conclusive evidence for a role in sex differences for systemic signals that originate from the CNS and the fat body, while the progenitor did potentially have some role in mitigating sex differences in the lymph gland. These results suggest that juxtacrine signals or perhaps cell autonomous signals play an important mechanistic role in sex differences in hematopoiesis. However, this does not imply the absence of other known types of sex differences that have been demonstrated to exist in flies and that we did not assay for, such as differences in physiology or metabolism (64). Instead, our work assayed cell numbers, a parameter which is most relevant for immune function. As the repertoire of known sex differences in hematopoiesis grows, which we

predict will be the case once separating data by sex becomes the norm in the field, it will be valuable to revisit the role of systemic signals as these are likely to play a part in at least some of these additional processes.

In the adult fly, there are intriguing sex-specific behavioural responses to the presence of bacteria. For example, female flies are less likely to lay eggs in the presence of high levels of bacteria, seen as a protective mechanism designed to avoid egg laying in an environment inhospitable to them (59). In the larval stage it is less clear what sex-differences are meant to accomplish. It could be that their role is to set up future differences in the adult, and/or it could be that there is emphasis on preventing infection that could become chronic and harm egg production. The possibility of sex-differences in larva impacting the adult immune response is supported by noting that a large portion of adult hemocytes derive from the larval lymph gland (65). The potential importance of preventing infection in females in larva is highlighted by studies showing that infection in adult female flies impacts egg production and/or fecundity (66,67).

Taken as a whole our work highlights the complex interactions between sex, genotype, and the environment in controlling fly hematopoiesis and immunity. Our phenotypic analysis shows substantial variation across genotypes and environmental conditions in the proportion of different populations in the lymph gland. In some experiments this did not allow us to obtain conclusive findings. However, this variability could represent important individual differences in life history, growth conditions, and environmental conditions between larvae. By accounting for sex as a factor that impacts lymph gland

phenotype in future work it should be possible to reduce variation introduced by mixing data from males and females. This will improve reproducibility and make future analysis more precise and meaningful.

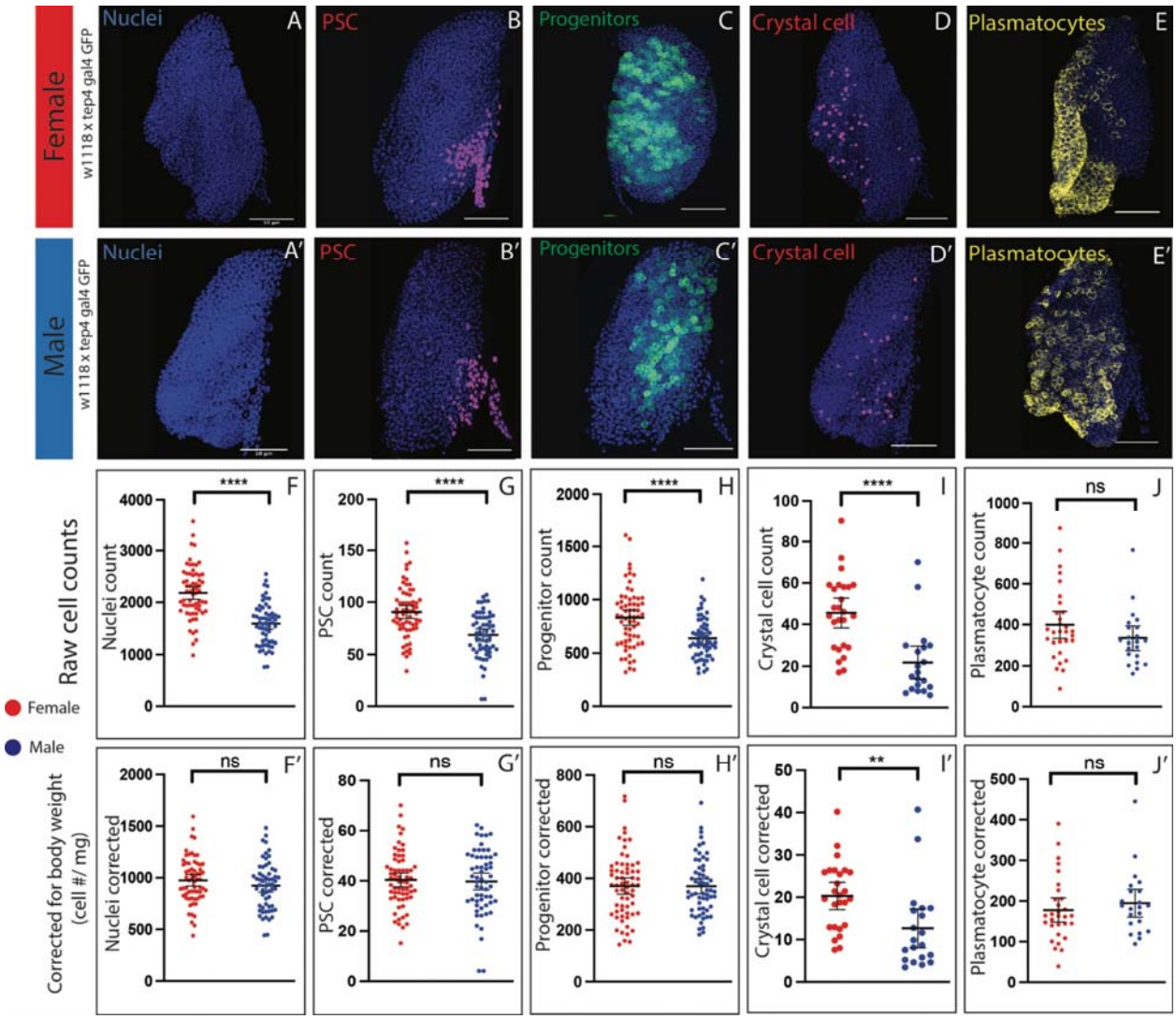

Figure 1- Characterizing sex differences in the lymph gland (A-E') Representative images of female (A-E) and male (A'-E') *w^{1118} x tep4-gal4; UAS-GFP* lymph glands stained with ToPro, Antp (B, B') to mark for PSC cells, endogenously expressing GFP in tep4+ cells (C, C') to mark progenitors, Hnt (D, D') to mark for crystal cells, and P1 (E, E') to mark for plasmatocytes. (F-J) Raw cell counts plotted for both males and females. (F) Raw number of nuclei, used to measure organ size, plotted for males and females (female n=64, male n=59, p<0.0001). (G) Raw number of PSC cells (Antp+), plotted for males and females (female n=64, male n=59, p<0.0001). (H) Raw number of progenitors (tep4+), plotted for males and females (female n=64, male n= 59, p<0.0001). (I) Raw number of crystal cells (Hnt+), plotted for males and females (female n=25, male n=19, p<0.0001). (J) Raw number of plasmatocytes (P1+), plotted for males and females (female n=30, male n=22, p=0.1661). (F'-J') Corrected for body weight by dividing each female data point by 2.24mg and dividing each male data point by 1.72mg. (F') Corrected nuclei count, used to measure organ size (female n=64, male n=59, p=0.2107). (G') Corrected number of

PSC cells (Antp+) (female n=64, male n=59, p=0.7819). (H’) Corrected number of progenitors (tep4+) (female n=64, male n=59, p=0,9705). (I’) Corrected number of crystal cells (Hnt+) (female n=25, male n=19, p=0.0056). (J’) Corrected number of plasmatocytes (P1+) (female n=30, male n=22, p=0.4531). **** indicates P<0.0001, *** indicates P<0.001, ** indicates P<0.01, * indicates P<0.05, ns (non-significant) indicates P>0.05. Error bars are 95% CI.

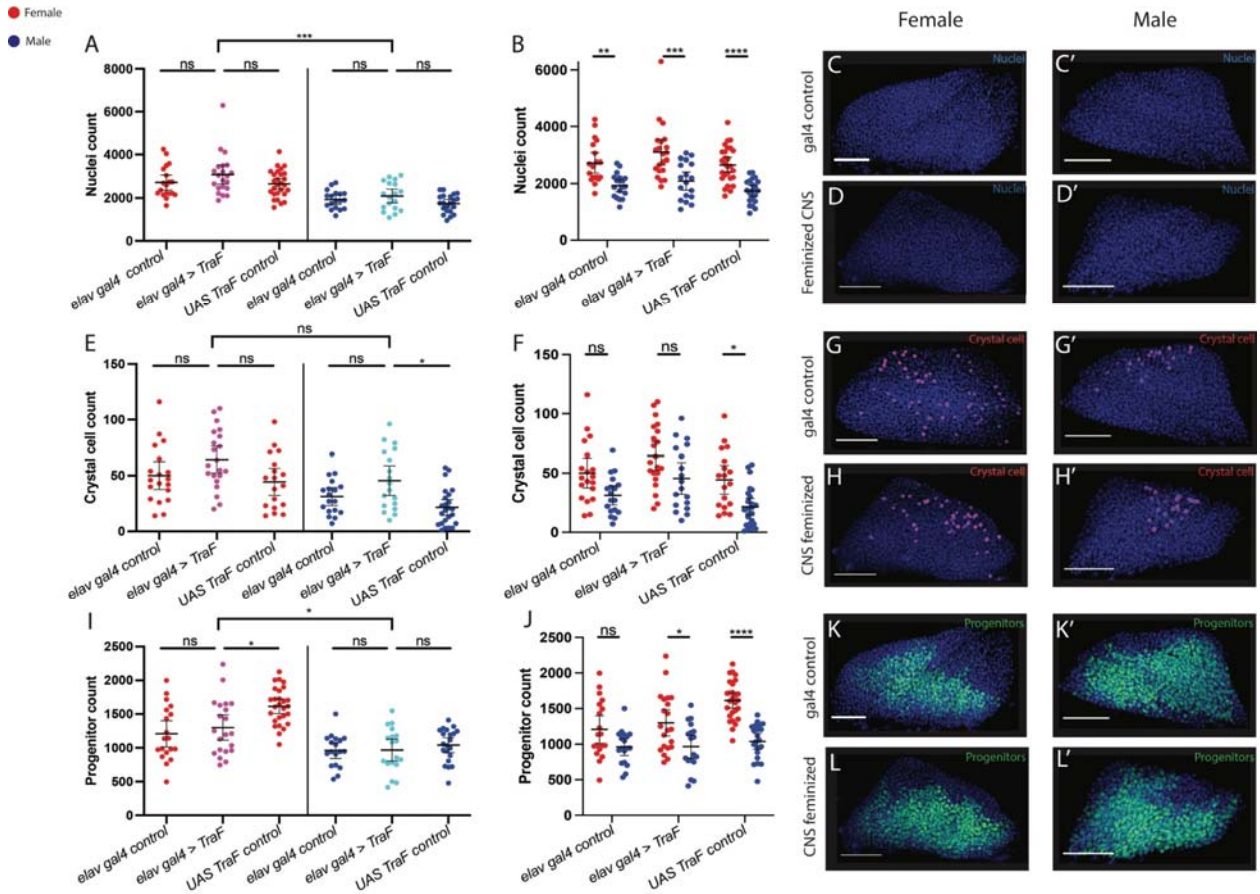

Figure 2- Feminizing the CNS (A-B) Raw cell counts for total number of nuclei, stained with ToPro. Quantification using a two-way ANOVA, post-hoc Tukey's test for: *elav-Gal4* control females (n=19), *elav-Gal4>Tra^F* females (n=21), *UAS Tra^F* control females (n=27), *elav-Gal4* control males (n=18), *elav-Gal4>Tra^F* males (n=18), *UAS Tra^F* control males (n=21). The genotype:sex interaction constant was not significant (p=0.8059). (C) Representative image of *elav-Gal4* control female stained with Topro. (C') Representative image of *elav-Gal4* control male stained with ToPro. (D,D') Representative image of *elav-Gal4;domeMESO GFP > UAS Tra^F* female (D) and male (D') stained with ToPro. (E-F) Raw cell counts for total number of crystal cells, stained with Hnt. Quantification using a two-way ANOVA, post-hoc Tukey's test for: *elav-Gal4* control females(n=19), *elav-Gal4 > Tra^F* females(n=21), *UAS Tra^F* control females(n=18), *elav-Gal4* control males(n=18), *elav-Gal4 > Tra^F* males(n=18), *UAS Tra^F* control males(n=24) The genotype:sex interaction constant was not significant (p=0.8966). (G, G') Representative image of *elav-Gal4* control female (G) and male (G') stained with Hnt. (H, H') Representative image of *elav-Gal4;domeMESO GFP > UAS Tra^F* female (H) and male (H') stained with Hnt. (I-J) Raw cell counts for total number of progenitors, expressing GFP in domeMESO+ cells. Quantification using a two-way ANOVA, post-hoc Tukey's test, for: *elav-Gal4* control females (n=19), *elav-Gal4 > Tra^F* females(n=21), *UAS Tra^F* control females(n=27), *elav-Gal4* control males (n=18), *elav-*

Gal4 >Tra^{F} males (n=18), *UAS Tra*^{F} control males (n=21) The genotype:sex interaction constant was not significant (p=0.0542). (K, K') Representative image of *elav-Gal4* control female (K) and male (K'), expressing GFP in domeMESO+ cells. (L, L') Representative image of *elav-Gal4;domeMESO GFP > UAS Tra*^{F} female (L) and male (L'), expressing GFP in domeMESO+ cells. **** indicates P<0.0001, *** indicates P<0.001, ** indicates P<0.01, * indicates P<0.05, ns (non-significant) indicates P>0.05. Error bars indicate 95% CI.

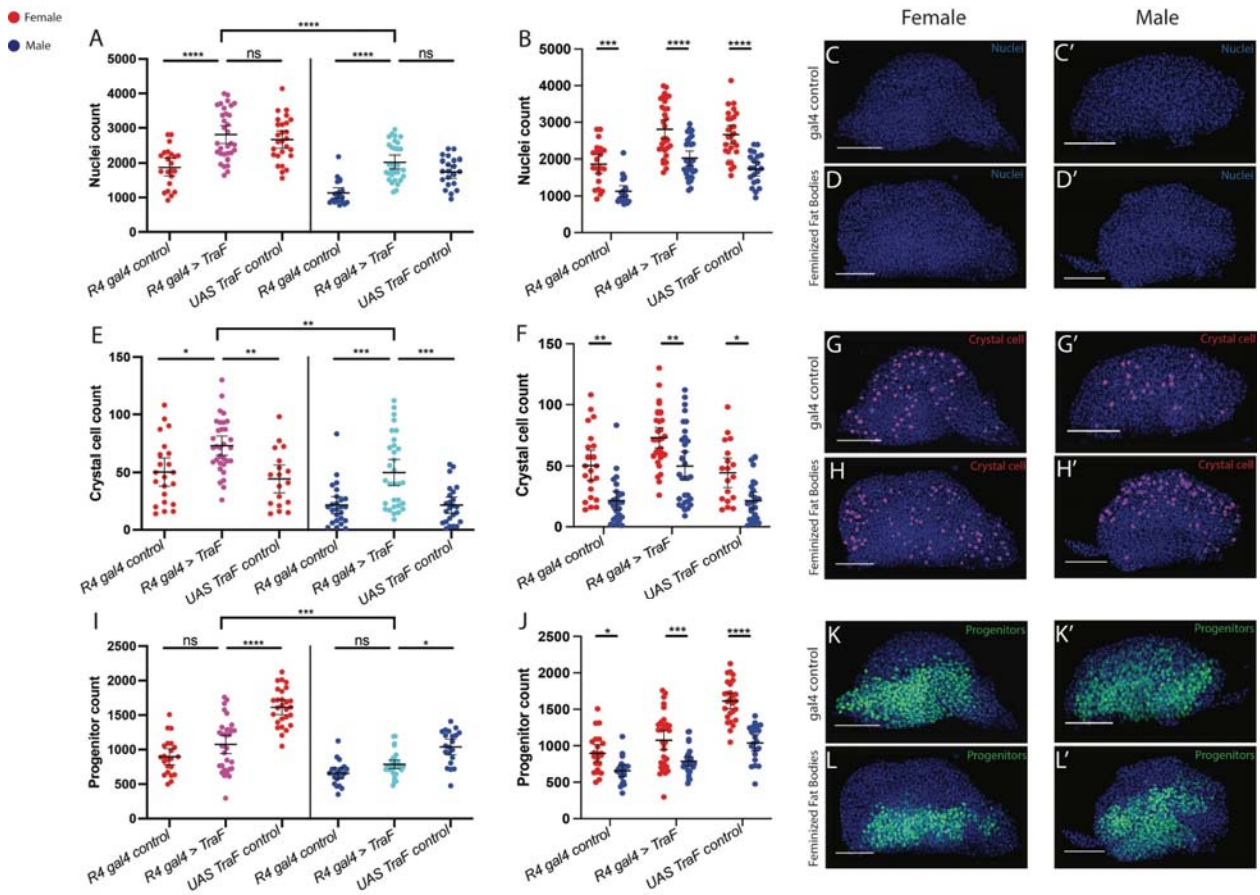

Figure 3- Feminizing the fat bodies (A-B) Raw cell counts for total number of nuclei, stained with ToPro. Quantification using a two-way ANOVA, post-hoc Tukey's test, for: *R4-Gal4* female control (n=22), *R4-Gal4* feminized females (n=32), *UAS Tra*^{F} control females (n=27), *R4-Gal4* control males (n=21),*R4-Gal4* feminized males (n=31), *UAS Tra*^{F} control males (n=21). The genotype:sex interaction constant was not significant (p=0.7379). (C, C') Representative image of *R4-Gal4* control female (C) and male (C') stained with Topro. (D) Representative image of *R4-Gal4;domeMESO GFP < UAS Tra*^{F} feminized female stained with ToPro. (D') Representative image of *R4-Gal4;domeMESO GFP < UAS Tra*^{F} feminized male stained with ToPro. (E-F) Raw cell counts for total number of crystal cells, stained with Hnt. Quantification using a two-way ANOVA, post-hoc Tukey's test, for: *R4-Gal4* control (n=22), *R4-Gal4* feminized females (n=32), *UAS Tra*^{F} control (n=18), *R4-Gal4* control males (n=25), *R4-Gal4* feminized males (n=31), *UAS Tra*^{F} control males (n=24). The genotype:sex interaction constant was no significant (p=0.7910). (G, G') Representative image of *R4-Gal4* control female (G) and male (G') stained with Hnt. (H) Representative image of *R4-Gal4;domeMESO GFP x UAS Tra*^{F} feminized female stained with Hnt. (H') Representative image of *R4-Gal4;domeMESO GFP x UAS Tra*^{F} feminized male stained with Hnt. (I-J) Raw cell counts for total number of progenitors, expressing GFP in domeMESO+ cells. Quantification using a two-way ANOVA, post-hoc Tukey's test, for: *R4-Gal4* control females

(n=22), *R4-Gal4* feminized females (n=32), *UAS Tra*^{F} control females(n=27), *R4-Gal4* control males (n=21), *R4-Gal4* feminized males (n=31), *UAS Tra*^{F} control males(n=21). The genotype:sex interaction constant was significant (p=0.0045). (K, K') Representative image of *R4-Gal4* control female (K) and male (K'), expressing GFP in domeMESO+ cells. (L) Representative image of *R4-Gal4;domeMESO GFP x UAS Tra*^{F} feminized female, expressing GFP in domeMESO+ cells. (L') Representative image of *R4-Gal4;domeMESO GFP x UAS Tra*^{F} feminized male, expressing GFP in domeMESO+ cells.**** indicates P<0.0001, *** indicates P<0.001, ** indicates P<0.01, * indicates P<0.05, ns (non-significant) indicates P>0.05. Error bars indicate 95% CI.

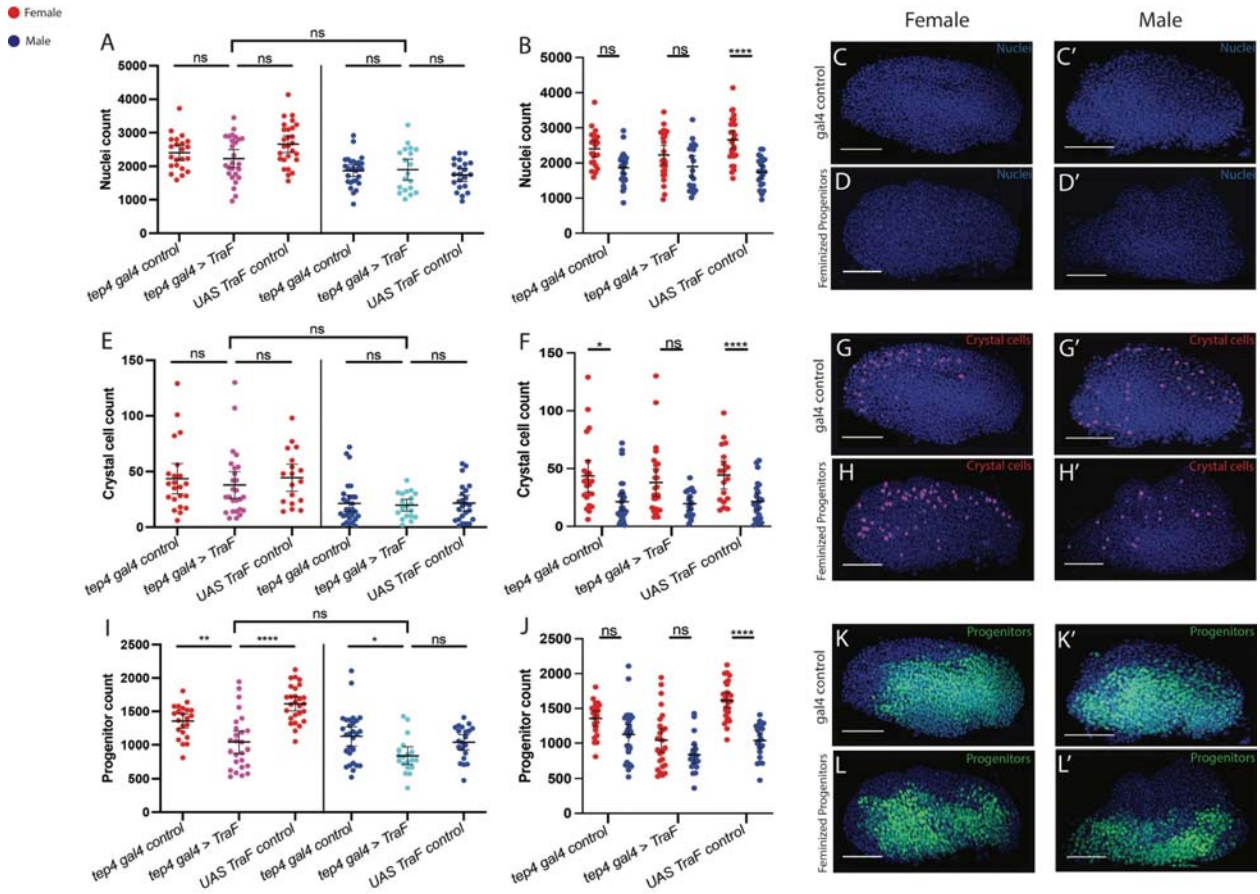

Figure 4- Feminizing the progenitors (A-B) Raw cell counts for total number of nuclei, stained with ToPro. Quantification using a two-way ANOVA, post-hoc Tukey's test, for: *tep4-Gal4* control females (n=22), *tep4-Gal4* feminized females (n=26), *UAS Tra^F* control females (n=27), *tep4-Gal4* control males (n=28), *tep4-Gal4* feminized males (n=19), *UAS Tra^F* control males (n=21). The genotype:sex interaction constant was significant (p=0.0379). (C, C') Representative image of *tep4-Gal4* control female (C) and male (C') stained with Topro. (D, D') Representative image of *tep4-Gal4;domeMESO GFP < UAS Tra^F* feminized female (D) and male (D') stained with ToPro. (E-F) Raw cell counts for total number of crystal cells, stained with Hnt. Quantification using a two-way ANOVA, post-hoc Tukey's test, for: *tep4-Gal4* control females (n=22), *tep4-Gal4* feminized females (n=26), *UAS Tra^F* control females (n=18), *tep4-Gal4* control males (n=28), *tep4-Gal4* feminized males (n=19), *UAS Tra^F* control males (n=24). The genotype:sex interaction constant was not significant (p=0.8740). (G) Representative image of *tep4-Gal4* control female stained with Hnt. (G') Representative image of *tep4gal4* control male stained with Hnt. (H) Representative image of *tep4-Gal4;domeMESO GFP x UAS Tra^F* feminized female stained with Hnt. (H') Representative image of *tep4-Gal4;domeMESO GFP x UAS Tra^F* feminized male stained with Hnt. (I-J) Raw cell counts for total number of progenitors, expressing GFP in domeMESO+ cells. Quantification using a two-way ANOVA, post-hoc Tukey's test, for: *tep4-Gal4* control females (n=22),

tep4-Gal4 feminized females (n=26), *UAS Tra*^{F} control females (n=27), t*ep4-Gal4* control males (n=28), *tep4-Gal4* feminized males (n=19), *UAS Tra*^{F} control males (n=21). The genotype:sex interaction constant was significant (p=0.0069) (K) Representative image of *tep4-Gal4* control female, expressing GFP in domeMESO+ cells. (K') Representative image of *tep4-Gal4* control male, expressing GFP in domeMESO+ cells. (L) Representative image of *tep4-Gal4;domeMESO GFP x UAS Tra*^{F} feminized female, expressing GFP in domeMESO+ cells. (L') Representative image of *tep4-Gal4;domeMESO GFP x UAS Tra*^{F} feminized male, expressing GFP in domeMESO+ cells. **** indicates P<0.0001, *** indicates P<0.001, ** indicates P<0.01, * indicates P<0.05, ns (non-significant) indicates P>0.05. Error bars indicate 95% CI.

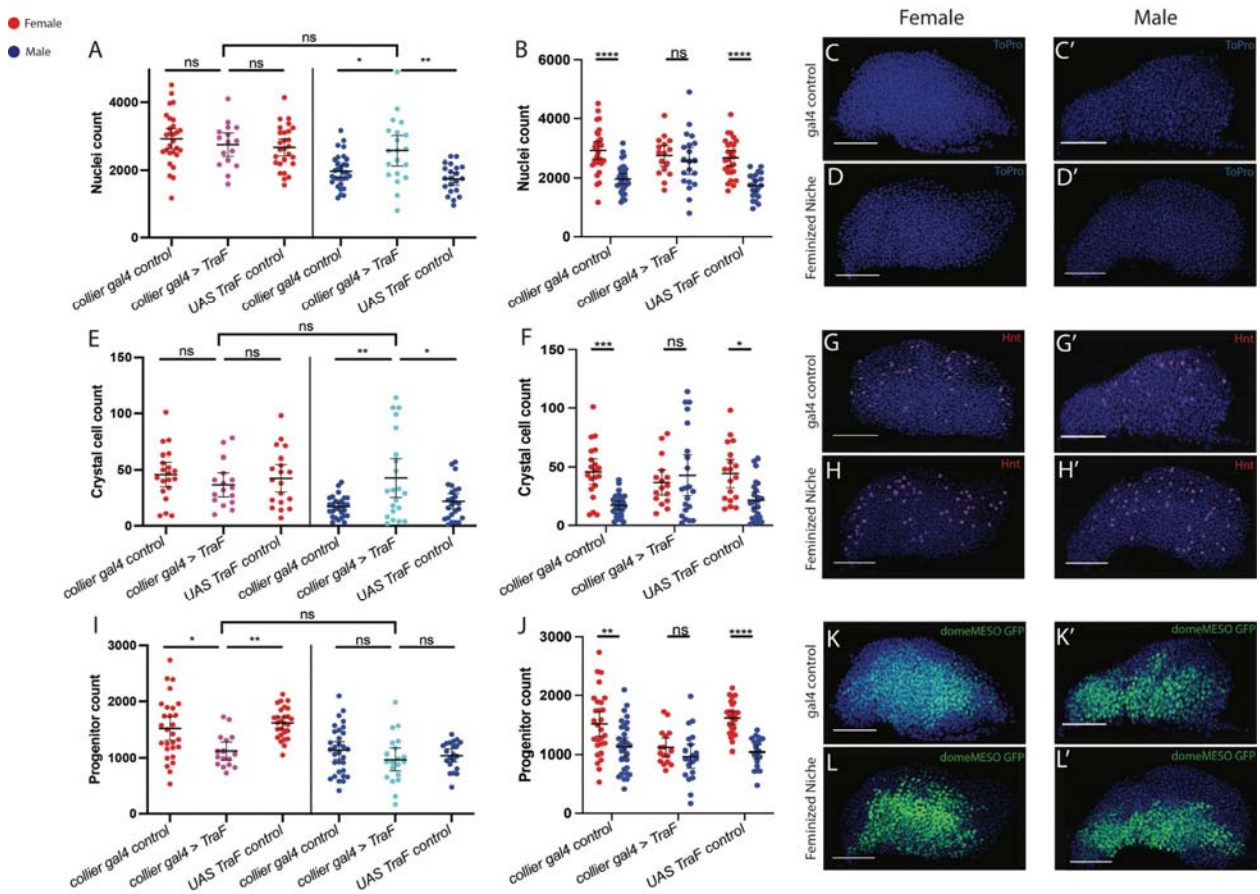

Figure 5- Feminizing the PSC (A-B) Raw cell counts for total number of nuclei, stained with ToPro. Quantification using a two-way ANOVA, post-hoc Tukey's test, for: *collier-Gal4* control females (n=28), *collier-Gal4* feminized females (n=16), *UAS Tra^F* control females (n=27), *collier-Gal4* control males(n=31), *collier-Gal4* feminized males(n=20), *UAS Tra^F* control males (n=21). The genotype:sex interaction constant was significant (p=0.0139). (C, C') Representative image of *collier-Gal4* control female (C) and male (C') stained with Topro. (D) Representative image of *collier-Gal4;domeMESO GFP < UAS Tra^F* feminized female stained with ToPro. (D') Representative image of *collier-Gal4;domeMESO GFP < UAS Tra^F* feminized male stained with ToPro. (E-F) Raw cell counts for total number of crystal cells, stained with Hnt. Quantification using a two-way ANOVA, post-hoc Tukey's test, for: *collier-Gal4* control females (n=20), *collier-Gal4* feminized females (n=16), *UAS Tra^F* control females (n=18), *collier-Gal4* control males (n=29), *collier-Gal4* feminized males (n=21), *UAS Tra^F* control males (n=24). The genotype:sex interaction constant was significant (p=0.0022). (G, G') Representative image of *collier-Gal4* control female (G) and male (G') stained with Hnt. (H) Representative image of *collier-Gal4;domeMESO GFP x UAS Tra^F* feminized female stained with Hnt. (H') Representative image of *collier-Gal4;domeMESO GFP x UAS Tra^F* feminized male stained with Hnt. (I-J) Raw cell counts for total number of progenitors, expressing GFP in domeMESO+ cells. Quantification using a two-way

ANOVA, post-hoc Tukey's test, for: *collier-Gal4* control females (n=28), *collier-Gal4* feminized females (n=16), *UAS Tra*^{F} control females (n=27), *collier-Gal4* control males (n=31), *collier-Gal4* feminized males (n=20), *UAS Tra*^{F} control males (n=21) and *collier-Gal4* feminized males (p=0.9910). The genotype:sex interaction constant was not significant (p=0.0529). (K, K') Representative image of *collier-Gal4* control female (K) and male (K'), expressing GFP in domeMESO+ cells. (L) Representative image of *collier-Gal4;domeMESO GFP x UAS Tra*^{F} feminized female, expressing GFP in domeMESO+ cells. (L') Representative image of *collier-Gal4;domeMESO GFP x UAS Tra*^{F} feminized male, expressing GFP in domeMESO+ cells.**** indicates P<0.0001, *** indicates P<0.001, ** indicates P<0.01, * indicates P<0.05, ns (non-significant) indicates P>0.05. Error bar indicates 95% CI.

	Nuclei	**Crystal cells**	**Progenitors**
Feminized CNS (Fig 2)	**0.8059**	**0.8966**	**0.0542**
Feminized FB (Fig 3)	**0.7379**	**0.7910**	**0.0045**
Feminized Progenitors (Fig 4)	**0.0379**	**0.8740**	**0.0069**
Feminized Niche (Fig 5)	**0.0139**	**0.0022**	**0.0529**

Table 1- Interaction constants for feminization experiments Sex:Genotype interaction constants derived from two-way ANOVA, post-hoc Tukey's test performed on data from Figures 2-5(see methods). Significant interaction constant highlighted in yellow(p<0.05).

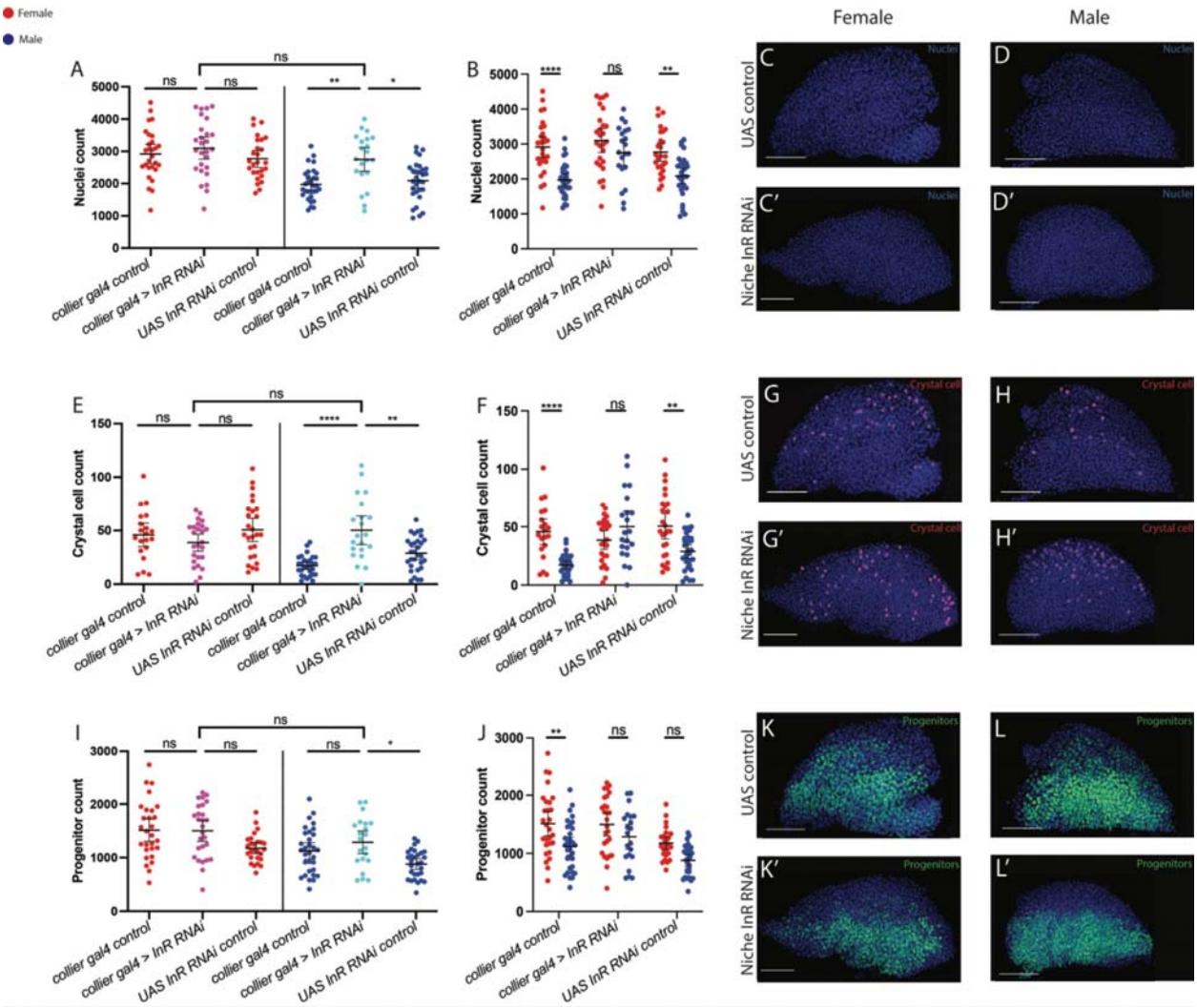

Figure 6- Knocking down insulin signaling in the PSC (A-B) Raw cell counts for total number of nuclei, stained with ToPro. Quantification using a two-way ANOVA, post-hoc Tukey's test, for: *collier-Gal4* control females (n=28), *collier-Gal4>InR RNAi* females (n=27), *UAS InR RNAi* females (n=26), *collier-Gal4* control males (n=31), *collier-Gal4>InR RNAi* males (n=21), *UAS InR RNAi* control males (n=30). The sex:genotype interaction constant was not significant (p=0.0931). (C) Representative image of +> *UAS InR RNAi* control females stained with ToPro. (C') Representative image of *collier-Gal4 > UAS InR RNAi* female stained with ToPro. (D) Representative image of +> *UAS InR RNAi* control male stained with ToPro, (D') Representative image of *collier-Gal4 > UAS InR RNAi* male stained with ToPro. (E-F) Raw cell counts for total number of crystal cells, stained with Hnt. A two-way ANOVA, post-hoc Tukey's test, for: *collier-Gal4* control females (n=20), *collier-Gal4>InR RNAi* females (n=25), *UAS InR RNAi* females (n=26), *collier-Gal4* control males (n=30), *collier-Gal4>InR RNAi* males (n=21), *UAS InR RNAi* control males (n=30). The sex:genotype interaction constant was significant (p<0.0001). (G)

Representative image of +> *UAS InR RNAi* control females stained with Hnt. (G') Representative image of *collier-Gal4* > *UAS InR RNAi* female stained with Hnt. (H) Representative image of +> *UAS InR RNAi* control male stained with Hnt (H') Representative image of *collier-Gal4* > *UAS InR RNAi* male stained with Hnt. (I-J) Raw cell counts for total number of progenitors, expressing GFP in domeMESO+ cells. A two-way ANOVA, post-hoc Tukey's test, for: *collier-Gal4* control females (n=28), *collier-Gal4>InR RNAi* females (n=27), *UAS InR RNAi* females (n=26), *collier-Gal4* control males (n=31), *collier-Gal4>InR RNAi* males (n=21), *UAS InR RNAi* control males (n=30). The genotype:sex interaction constant was not significant (p=0.5419). (K) Representative image of +> *UAS InR RNAi* control females expressing GFP in domeMESO+ cells. (K') Representative image of *collier-Gal4* > *UAS InR RNAi* female expressing GFP in domeMESO+ cells. (L) Representative image of +> *UAS InR RNAi* control male expressing GFP in domeMESO+ cells. (L') Representative image of *collier gal4* > *UAS InR RNAi* male expressing GFP in domeMESO+ cells.**** indicates P<0.0001, *** indicates P<0.001, ** indicates P<0.01, * indicates P<0.05, ns (non-significant) indicates P>0.05. Error bar indicates 95% CI.

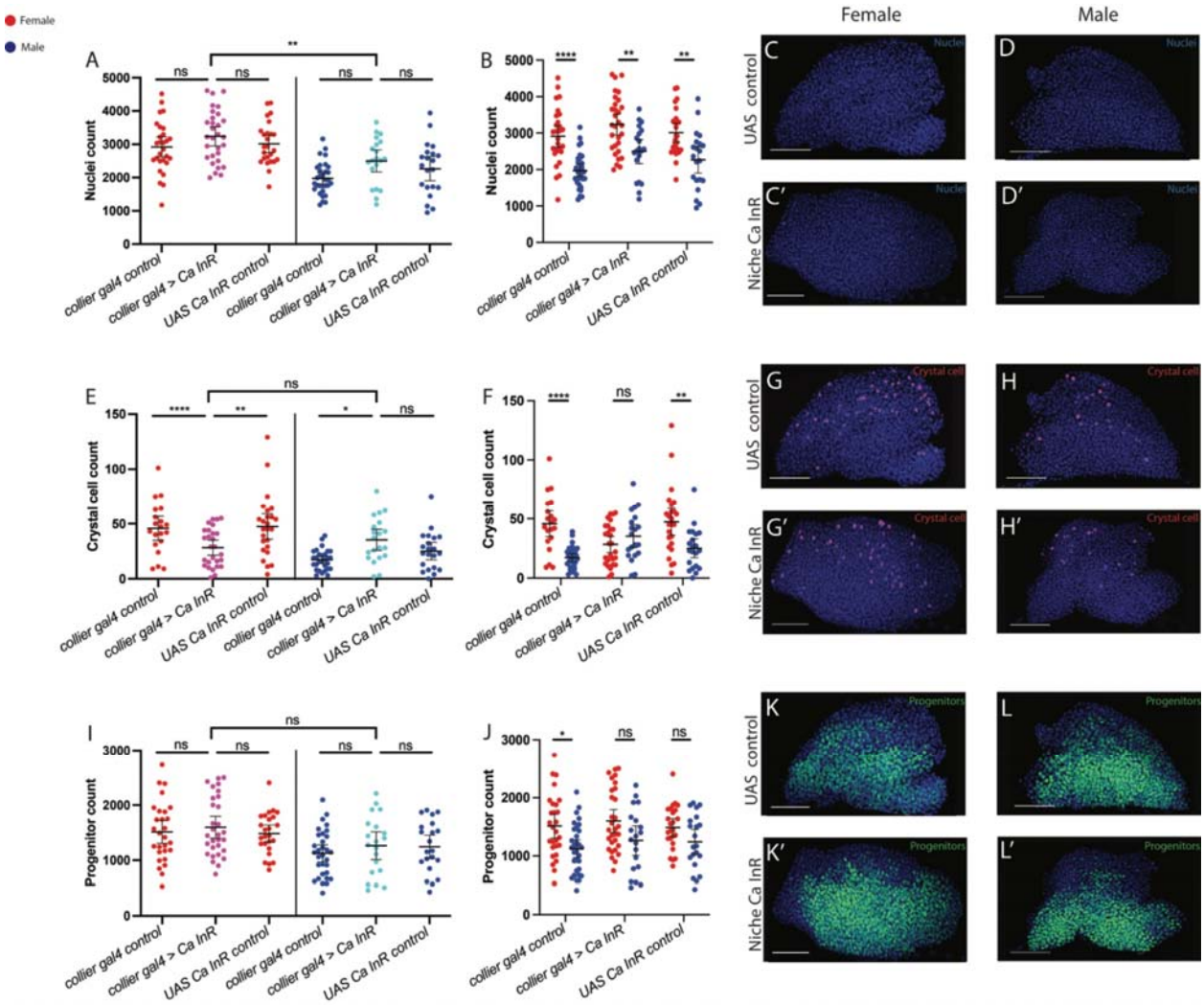

Figure 7- Constitutively activating insulin in the PSC (A-B) Raw cell counts for total number of nuclei, stained with ToPro. Quantification using a two-way ANOVA, post-hoc Tukey's test, for: *collier-Gal4* control females (n=28), *collier-Gal4>Ca InR* females (n=30), *UAS Ca InR* control females (n=25), *collier-Gal4* control males (n=31), *collier-Gal4>Ca InR* males (n=20), *UAS Ca InR* control males (n=21). The genotype:sex interaction constant was no significant (p=0.6852). (C) Representative image of +> *UAS Ca InR* control females stained with ToPro. (C') Representative image of *collier-Gal4 > UAS Ca InR* female stained with ToPro. (D) Representative image of +> *UAS Ca InR* control male stained with ToPro, (D') Representative image of *collier-Gal4 > UAS Ca InR* male stained with ToPro. (E-F) Raw cell counts for total number of crystal cells, stained with Hnt. Quantification using a two-way ANOVA, post-hoc Tukey's test, for: *collier-Gal4* control females (n=20), *collier-Gal4>Ca InR* females (n=27), *UAS Ca InR* females (n=25), *collier-Gal4* control males (n=30), *collier-Gal4>Ca InR* males (n=20), *UAS Ca InR* control males (n= 21). The genotype:sex interaction constant was significant (p<0.0001). (G) Representative image of +> *UAS Ca InR* control females stained with Hnt. (G') Representative image of

collier-Gal4 > UAS Ca InR female stained with Hnt. (H) Representative image of +> *UAS Ca InR* control male stained with Hnt (H') Representative image of *collier-Gal4 > UAS Ca InR* male stained with Hnt. (I-J) Raw cell counts for total number of progenitors, expressing GFP in domeMESO+ cells. Quantification using a two-way ANOVA, post-hoc Tukey's test, for:*collier-Gal4* control females (n=28), *collier-Gal4>Ca InR* females (n=30), *UAS Ca InR* control females (n=25), *collier-Gal4* control males (n=31), *collier-Gal4>Ca InR* males (n=20), *UAS Ca InR* control males (n=21). The genotype:sex interaction constant was not significant (p=0.7455). (K) Representative image of +> *UAS Ca InR* control females expressing GFP in domeMESO+ cells. (K') Representative image of *collier-Gal4 > UAS Ca InR* female expressing GFP in domeMESO+ cells. (L) Representative image of +> *UAS Ca InR* control male expressing GFP in domeMESO+ cells. (L') Representative image of *collier-Gal4 > UAS Ca InR* male expressing GFP in domeMESO+ cells.**** indicates P<0.0001, *** indicates P<0.001, ** indicates P<0.01, * indicates P<0.05, ns (non-significant) indicates P>0.05. Error bar indicates 95% CI.

	Nuclei	**Crystal cells**	**Progenitors**
InR RNAi	**0.0931**	**<0.0001**	**0.5789**
Ca InR	**0.6852**	**<0.0001**	**0.7455**

Table 2- Interaction constants for insulin modulation Sex:Genotype interaction constants derived from two-way ANOVA, post-hoc Tukey's test performed on data from Figures 6-7(see methods). Significant interaction constant highlighted in yellow(p<0.05).

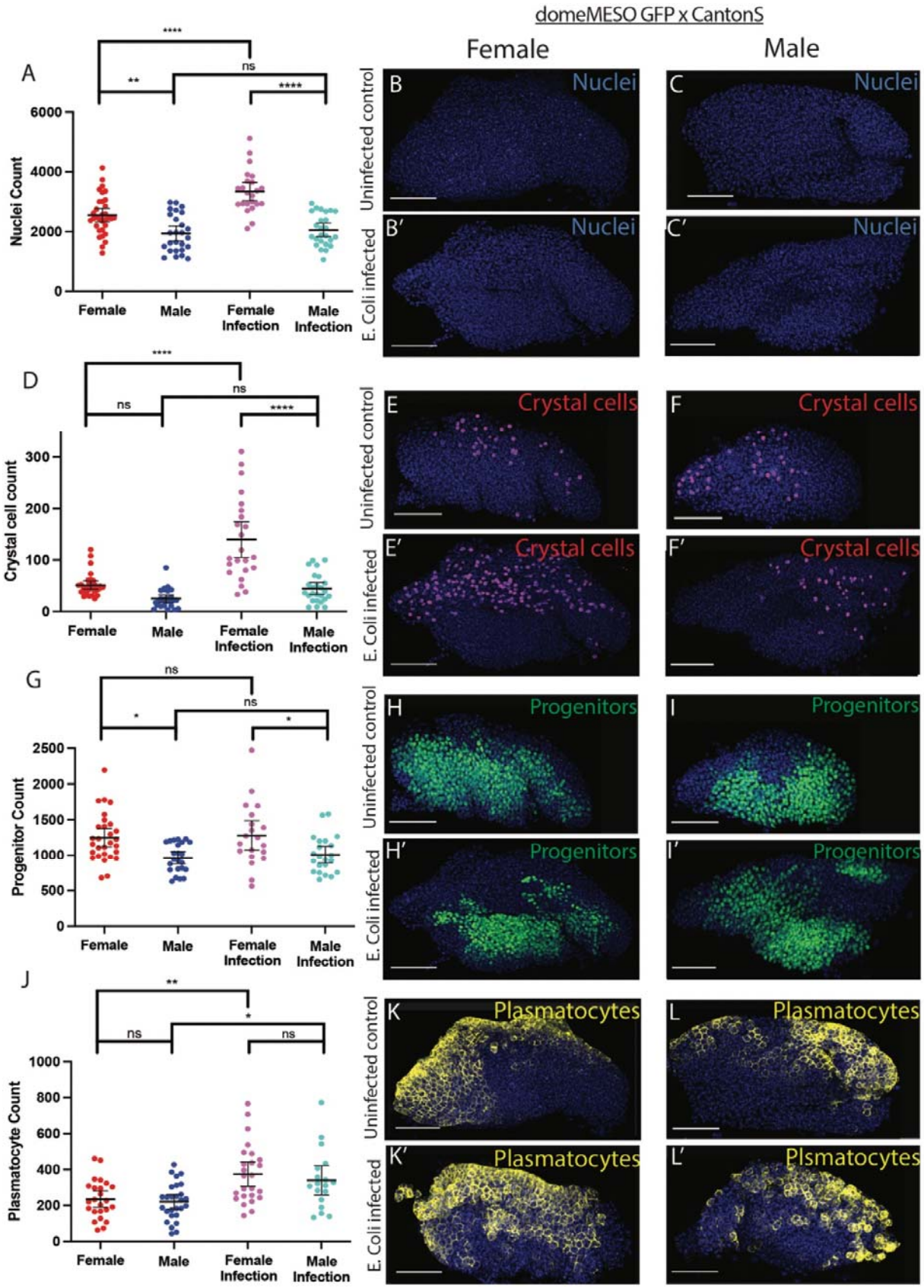
domeMESO GFP x CantonS
Female
Male
A
Nuclei Count
6000
4000
2000
0
Female
Male
Female Infection
Male Infection
****
**
ns
****
B
Nuclei
C
Nuclei
B′
Nuclei
C′
Nuclei
Uninfected control
E. Coli infected
D
Crystal cell count
300
200
100
0
ns
ns
****
E
Crystal cells
F
Crystal cells
E′
Crystal cells
F′
Crystal cells
G
Progenitor Count
2500
2000
1500
1000
500
0
ns
ns
*
*
H
Progenitors
I
Progenitors
H′
Progenitors
I′
Progenitors
J
Plasmatocyte Count
1000
800
600
400
200
0
**
*
ns
ns
K
Plasmatocytes
L
Plasmatocytes
K′
Plasmatocytes
L′
Plsmatocytes

Figure 8- Infection with E. Coli (A) Raw cell counts for total number of nuclei, stained with ToPro, in *domeMESO GFP x CantonS* flies both uninfected (female n=33, male n=26) and infected with *E.coli* bacteria (female n=23, male n=25). (B, B') Representative image of an uninfected (B) and infected (B') female lymph gland stained with ToPro. (C, C') Representative image of uninfected (C) and infected (C') male lymph gland stained with ToPro. (D) Raw cell counts for total number of crystal cells in *domeMESO GFP x CantonS* flies both uninfected (female n=33, male n=26) and infected with *E.coli* bacteria (female n=23, male n=25). (E, E') Representative image of an uninfected (E) and infected (E') female lymph gland stained with Hnt. (F, F') Representative image of an uninfected (F) and infected (F') male lymph gland stained with Hnt. (G) Raw cell counts for total number of progenitors, expressing GFP in domeMESO+ cells, in *domeMESO GFP x CantonS* flies both uninfected (female n=29, male n=23) and infected with *E.coli* bacteria (female n=20, male n=22). (H, H') Representative image of an uninfected (H) and infected (H') female lymph gland expressing GFP in domeMESO+ cells. (I, I') Representative image of an uninfected male (I) and infected (I') lymph gland expressing GFP in domeMESO+ cells. (J) Raw cell counts for total number of plasmatocytes, stained with P1, in *domeMESO GFP x CantonS* flies both uninfected (female n=24, male n=27) and infected with *E.coli* bacteria (female n=25, male n=18). (K, K') Representative image of an uninfected (K) and infected (K') female lymph gland stained with P1. (L, L') Representative image of an uninfected (L) and infected (L') male lymph gland stained with P1. All quantification done using a one-way ANOVA, post-hoc Tukey's test. **** indicates P<0.0001, *** indicates P<0.001, ** indicates P<0.01, * indicates P<0.05, ns (non-significant) indicates P>0.05. Error bar indicates 95% CI.

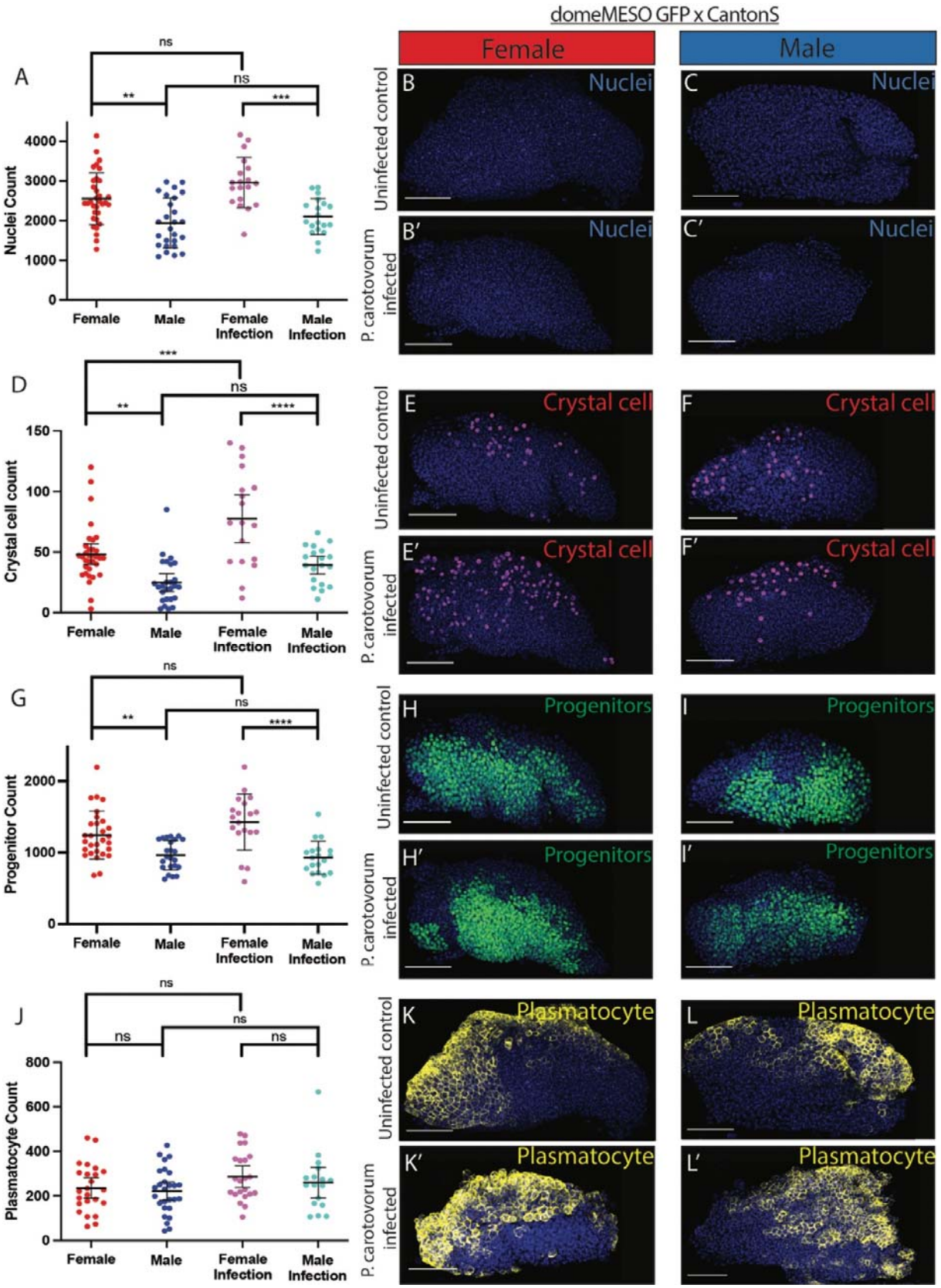
domeMESO GFP x CantonS
Female
Male
A
ns
ns
**
***
Nuclei Count
4000
3000
2000
1000
0
Female
Male
Female Infection
Male Infection
Uninfected control
P. carotovorum infected
B
Nuclei
C
Nuclei
B′
Nuclei
C′
Nuclei
D
***
ns
**
****
Crystal cell count
150
100
50
0
E
Crystal cell
F
Crystal cell
E′
Crystal cell
F′
Crystal cell
G
ns
ns
**
****
Progenitor Count
2000
1000
0
H
Progenitors
I
Progenitors
H′
Progenitors
I′
Progenitors
J
ns
ns
ns
ns
Plasmatocyte Count
800
600
400
200
0
K
Plasmatocyte
L
Plasmatocyte
K′
Plasmatocyte
L′
Plasmatocyte

Figure 9- Infection with *P.carotovorum* (A) Raw cell counts for total number of nuclei, stained with ToPro, in *domeMESO GFP x CantonS* flies both uninfected (female n=33, male n=26) and infected with *P. carotovorum* bacteria (female n=19, male n=19). (B, B') Representative image of an uninfected (B) and infected (B') female lymph gland stained with ToPro. (C) Representative image of uninfected (C) and infected (C') male lymph gland stained with ToPro. (D) Raw cell counts for total number of crystal cells, stained with Hnt, in *domeMESO GFP x CantonS* flies both uninfected (female n=33, male n=26) and infected with *P.carotovorum* bacteria (female n=19, male n=19). (E, E') Representative image of an uninfected (E) and infected (E') female lymph gland stained with Hnt. (F, F') Representative image of an uninfected (F) and infected (F') male lymph gland stained with Hnt. (G)Raw cell counts for total number of progenitors, expressing GFP in domeMESO+ cells, in *domeMESO GFP x CantonS* flies both uninfected (female n=29, male n=23) and infected with *P. carotovorum* bacteria (female n=19, male n=19).(H, H') Representative image of an uninfected (H) and infected (H') female lymph gland expressing GFP in domeMESO+ cells. (I, I') Representative image of an uninfected (I) and infected (I') male lymph gland expressing GFP in domeMESO+ cells. (J) Raw cell counts for total number of plasmatocytes, stained with P1, in *domeMESO GFP x CantonS* flies both uninfected (female n=24, male n=27) and infected with *P. carotovorum* bacteria (female n=22, male n=17). (K) Representative image of an uninfected female lymph gland stained with P1. (K') Representative image of an infected female lymph gland stained with P1. (L) Representative image of an uninfected male lymph gland stained with P1. (L') Representative image of an infected male lymph gland stained with P1.
All quantification done using a one-way ANOVA, post-hoc Tukey's test. **** indicates P<0.0001, *** indicates P<0.001, ** indicates P<0.01, * indicates P<0.05, ns (non-significant) indicates P>0.05. Error bar indicates 95% CI.

References

1. Arnold, A.P. (2017), A general theory of sexual differentiation. Journal of Neuroscience Research, 95: 291-300. https://doi.org/10.1002/jnr.23884

2. Arnold, A. P. (2019). Rethinking sex determination of non-gonadal tissues. *Curr. Top. Dev. Biol.*134, 289-315. https://doi.org/10.1016/bs.ctdb.2019.01.003

3. Fairbairn, D. J. (2005). Allometry for sexual size dimorphism: Patterns and processes. Annual Review of Ecology, Evolution, and Systematics, 36(1), 51-71.

4.Zhang, H., Zhang, L., & He, Z. (2018). Sex-specific regulation of growth and muscle development in Drosophila melanogaster. Developmental Biology, 442(2), 136-147.

5. Bond, J. E., & Cormier, T. A. (2020). Hormonal regulation of sexual dimorphism in body size and tissue growth in Drosophila. Frontiers in Physiology, 11, 1013.

6. Hughes, I. A. (2001). Minireview: Sex differentiation. *Endocrinology*, *142*(8), 3281–3287. https://doi.org/10.1210/endo.142.8.8406

7. Wat, L. W., Chao, C., Bartlett, R., Buchanan, J. L., Millington, J. W., Chih, H. J., Chowdhury, Z. S., Biswas, P., Huang, V., Shin, L. J., Wang, L. C., Gauthier, M. L., Barone, M. C., Montooth, K. L., Welte, M. A., & Rideout, E. J. (2020). A role for triglyceride lipase brummer in the regulation of sex differences in Drosophila fat storage and breakdown. PLoS biology, 18(1), e3000595. https://doi.org/10.1371/journal.pbio.3000595

8. Hudry, B., Khadayate, S., & Miguel-Aliaga, I. (2016). The sexual identity of adult intestinal stem cells controls organ size and plasticity. Nature, 530(7590), 344–348.
https://doi.org/10.1038/nature16953

9. Mathews, K. W., Cavegn, M., & Zwicky, M. (2017). Sexual Dimorphism of Body Size Is Controlled by Dosage of the X-Chromosomal Gene Myc and by the Sex-Determining Gene tra in Drosophila. Genetics, 205(3), 1215–1228. https://doi.org/10.1534/genetics.116.192260

10. Surkova, S., Görne, J., Nuzhdin, S., & Samsonova, M. (2021). Interplay between sex determination cascade and major signaling pathways during Drosophila eye development: Perspectives for future research. Developmental biology, 476, 41–52. https://doi.org/10.1016/j.ydbio.2021.03.005

11. Dunn, S.E., Perry, W.A. & Klein, S.L. Mechanisms and consequences of sex differences in immune responses. *Nat Rev Nephrol* 20, 37–55 (2024). https://doi.org/10.1038/s41581-023-00787-w

12. Klein, S., Flanagan, K. Sex differences in immune responses. *Nat Rev Immunol* 16, 626–638 (2016). https://doi.org/10.1038/nri.2016.90

13. Meier, A., Chang, J. J., Chan, E. S., Pollard, R. B., Sidhu, H. K., Kulkarni, S., Wen, T. F., Lindsay, R. J., Orellana, L., Mildvan, D., Bazner, S., Streeck, H., Alter, G., Lifson, J. D., Carrington, M., Bosch, R. J., Robbins, G. K., & Altfeld, M. (2009). Sex differences in the Toll-like receptor-mediated response of

plasmacytoid dendritic cells to HIV-1. Nature medicine, 15(8), 955–959. https://doi.org/10.1038/nm.2004
14. Berghöfer, B., Frommer, T., Haley, G., Fink, L., Bein, G., & Hackstein, H. (2006). TLR7 ligands induce higher IFN-alpha production in females. Journal of immunology (Baltimore, Md. : 1950), 177(4), 2088–2096. https://doi.org/10.4049/jimmunol.177.4.2088
15. Boissier, J., Chlichlia, K., Digon, Y., Ruppel, A., & Moné, H. (2003). Preliminary study on sex-related inflammatory reactions in mice infected with Schistosoma mansoni. Parasitology research, 91(2), 144–150. https://doi.org/10.1007/s00436-003-0943-1
16. Melgert, B. N., Oriss, T. B., Qi, Z., Dixon-McCarthy, B., Geerlings, M., Hylkema, M. N., & Ray, A. (2010). Macrophages: regulators of sex differences in asthma?. American journal of respiratory cell and molecular biology, 42(5), 595–603. https://doi.org/10.1165/rcmb.2009-0016OC
17. Frisancho-Kiss, S., Davis, S. E., Nyland, J. F., Frisancho, J. A., Cihakova, D., Barrett, M. A., Rose,N. R., & Fairweather, D. (2007). Cutting edge: cross-regulation by TLR4 and T cell Ig mucin-3 determines sex differences in inflammatory heart disease. Journal of immunology (Baltimore, Md.: 1950), 178(11), 6710–6714. https://doi.org/10.4049/jimmunol.178.11.6710
18. Hewagama, A., Patel, D., Yarlagadda, S., Strickland, F. M., & Richardson, B. C. (2009). Stronger inflammatory/cytotoxic T-cell response in women identified by microarray analysis. Genes and immunity, 10(5), 509–516. https://doi.org/10.1038/gene.2009.12
19. Belmonte, R. L., Corbally, M.-K., Duneau, D. F., & Regan, J. C. (2020). Sexual dimorphisms in innate immunity and responses to infection in drosophila melanogaster. Frontiers in Immunology, 10. https://doi.org/10.3389/fimmu.2019.03075
20. Palmer WH, Medd NC, Beard PM, Obbard DJ. Isolation of a natural DNA virus of *Drosophila melanogaster*, and characterisation of host resistance and immune responses. *PLoS Pathog.* (2018) 14:e1007050. doi: 10.1371/journal.ppat.1007050
21. Chowdhury, M., Li, C.-F., He, Z., Lu, Y., Liu, X.-S., Wang, Y.-F., Ip, Y. T., Strand, M. R., & Yu, X.-Q. (2019). Toll family members bind multiple spätzle proteins and activate antimicrobial peptide gene expression in drosophila. Journal of Biological Chemistry, 294(26), 10172–10181. https://doi.org/10.1074/jbc.ra118.006804
22. Vincent, C. M., & Sharp, N. P. (2014). Sexual antagonism for resistance and tolerance to infection in Drosophila melanogaster. Proceedings. Biological sciences, 281(1788), 20140987. https://doi.org/10.1098/rspb.2014.0987
23. Duneau, D. F., Kondolf, H. C., Im, J. H., Ortiz, G. A., Chow, C., Fox, M. A., Eugénio, A. T., Revah, J., Buchon, N., & Lazzaro, B. P. (2017). The Toll pathway underlies host sexual dimorphism in resistance to both Gram-negative and Gram-positive bacteria in mated Drosophila. BMC biology, 15(1), 124. https://doi.org/10.1186/s12915-017-0466-3

24. Kutch, I. C., & Fedorka, K. M. (2017). A test for Y-linked additive and epistatic effects on surviving bacterial infections in Drosophila melanogaster. Journal of evolutionary biology, 30(7), 1400–1408. https://doi.org/10.1111/jeb.13118
25. Martins, N. E., Faria, V. G., Nolte, V., Schlötterer, C., Teixeira, L., Sucena, É., & Magalhães, S. (2014). Host adaptation to viruses relies on few genes with different cross-resistance properties. Proceedings of the National Academy of Sciences of the United States of America, 111(16), 5938–5943. https://doi.org/10.1073/pnas.1400378111
26. Ma, X., Li, W., Yu, H. *et al.* Bendless modulates JNK-mediated cell death and migration in *Drosophila*.*Cell Death Differ* 21, 407–415 (2014). https://doi.org/10.1038/cdd.2013.154
27. Kelsey, E. M., Luo, X., Brückner, K., & Jasper, H. (2012). Schnurri regulates hemocyte function to promote tissue recovery after DNA damage. *Journal of cell science*, *125*(Pt 6), 1393–1400. https://doi.org/10.1242/jcs.095323
28. Sinenko, S. A., Mandal, L., Martinez-Agosto, J. A., & Banerjee, U. (2009). Dual role of wingless signaling in stem-like hematopoietic precursor maintenance in drosophila. *Developmental Cell*, *16*(5), 756–763. https://doi.org/10.1016/j.devcel.2009.03.003
29. Pennetier, D., Oyallon, J., Morin-Poulard, I., Dejean, S., Vincent, A., & Crozatier, M. (2012). Size control of the Drosophila hematopoietic niche by bone morphogenetic protein signaling reveals parallels with mammals. *Proceedings of the National Academy of Sciences of the United States of America*, *109*(9), 3389–3394. https://doi.org/10.1073/pnas.1109407109
30. Lan, W., Liu, S., Zhao, L., & Su, Y. (2020). Regulation of Drosophila Hematopoiesis in Lymph Gland:From a Developmental Signaling Point of View. International journal of molecular sciences, 21(15), 5246. https://doi.org/10.3390/ijms21155246
31. Krzemień, J., Dubois, L., Makki, R., Meister, M., Vincent, A., & Crozatier, M. (2007). Control of blood cell homeostasis in Drosophila larvae by the posterior signalling centre. Nature, 446(7133), 325–328. https://doi.org/10.1038/nature05650
32. Mandal, L., Martinez-Agosto, J. A., Evans, C. J., Hartenstein, V., & Banerjee, U. (2007). A Hedgehog- and Antennapedia-dependent niche maintains Drosophila haematopoietic precursors. Nature, 446(7133), 320–324. https://doi.org/10.1038/nature05585
33. Morin-Poulard, I., Vincent, A., & Crozatier, M. (2013). The Drosophila JAK-STAT pathway in blood cell formation and immunity. JAK-STAT, 2(3), e25700. https://doi.org/10.4161/jkst.25700
34. Makki, R., Meister, M., Pennetier, D., Ubeda, J. M., Braun, A., Daburon, V., Krzemień, J., Bourbon, H. M., Zhou, R., Vincent, A., & Crozatier, M. (2010). A short receptor downregulates JAK/STAT signalling to control the Drosophila cellular immune response. *PLoS biology*, *8*(8), e1000441. https://doi.org/10.1371/journal.pbio.1000441
35. Mooney, R. A., Kulas, D. T., Bleyle, L. A., & Novak, J. S. (1997). The protein tyrosine phosphatase LAR has a major impact on insulin receptor

dephosphorylation. Biochemical and biophysical research communications, 235(3), 709–712. https://doi.org/10.1006/bbrc.1997.6889
36. Kulas, D. T., Goldstein, B. J., & Mooney, R. A. (1996). The transmembrane protein-tyrosine phosphatase LAR modulates signaling by multiple receptor tyrosine kinases. The Journal of biological chemistry, 271(2), 748–754. https://doi.org/10.1074/jbc.271.2.748
37. Tsujikawa, K., Kawakami, N., Uchino, Y., Ichijo, T., Furukawa, T., Saito, H., & Yamamoto, H. (2001). Distinct functions of the two protein tyrosine phosphatase domains of LAR (leukocyte common antigen-related) on tyrosine dephosphorylation of insulin receptor. Molecular endocrinology (Baltimore, Md.), 15(2), 271–280. https://doi.org/10.1210/mend.15.2.0592
38. Benmimoun, B., Polesello, C., Waltzer, L., & Haenlin, M. (2012). Dual role for Insulin/TOR signaling in the control of hematopoietic progenitor maintenance in Drosophila. Development (Cambridge, England), 139(10), 1713–1717. https://doi.org/10.1242/dev.080259
39. Kaur, H., Sharma, S. K., Mandal, S., & Mandal, L. (2019). Lar maintains the homeostasis of the hematopoietic organ in *drosophila* by regulating insulin signaling in the niche. *Development*, *146*(24). https://doi.org/10.1242/dev.178202
40. Handke, B., Poernbacher, I., Goetze, S., Ahrens, C. H., Omasits, U., Marty, F., Simigdala, N., Meyer, I., Wollscheid, B., Brunner, E., Hafen, E., & Lehner, C. F. (2013). The hemolymph proteome of fed and starved Drosophila larvae. PloS one, 8(6), e67208. https://doi.org/10.1371/journal.pone.0067208
41. Shim, J., Mukherjee, T., & Banerjee, U. (2012). Direct sensing of systemic and nutritional signals by haematopoietic progenitors in Drosophila. Nature cell biology, 14(4), 394–400. https://doi.org/10.1038/ncb2453
42. Cho, B., Spratford, C. M., Yoon, S., Cha, N., Banerjee, U., & Shim, J. (2018). Systemic control of immune cell development by integrated carbon dioxide and hypoxia chemosensation in Drosophila. Nature communications, 9(1), 2679. https://doi.org/10.1038/s41467-018-04990-3
43. Oyallon, J., Vanzo, N., Krzemień, J., Morin-Poulard, I., Vincent, A., & Crozatier, M. (2016). Two Independent Functions of Collier/Early B Cell Factor in the Control of Drosophila Blood Cell Homeostasis. *PloS one*, *11*(2), e0148978. https://doi.org/10.1371/journal.pone.0148978
44. Ferveur, J. F., Störtkuhl, K. F., Stocker, R. F., & Greenspan, R. J. (1995). Genetic feminization of brain structures and changed sexual orientation in male Drosophila. Science (New York, N.Y.), 267(5199), 902–905. https://doi.org/10.1126/science.7846534
45. Wat, L. W., Chao, C., Bartlett, R., Buchanan, J. L., Millington, J. W., Chih, H. J., Chowdhury, Z. S., Biswas, P., Huang, V., Shin, L. J., Wang, L. C., Gauthier, M. L., Barone, M. C., Montooth, K. L., Welte, M. A., & Rideout, E. J. (2020). A role for triglyceride lipase brummer in the regulation of sex differences in Drosophila fat storage and breakdown. PLoS biology, 18(1), e3000595. https://doi.org/10.1371/journal.pbio.3000595
46. Argue, K. J., & Neckameyer, W. S. (2014). Altering the sex determination pathway in Drosophila fat body modifies sex-specific stress responses. American

journal of physiology. Regulatory, integrative and comparative physiology, 307(1), R82–R92. https://doi.org/10.1152/ajpregu.00003.2014
47. Sethi, S., Lin, H. H., Shepherd, A. K., Volkan, P. C., Su, C. Y., & Wang, J. W. (2019). Social Context Enhances Hormonal Modulation of Pheromone Detection in Drosophila. Current biology : CB, 29(22), 3887–3898.e4. https://doi.org/10.1016/j.cub.2019.09.045
48. Hudry, B., Khadayate, S., & Miguel-Aliaga, I. (2016). The sexual identity of adult intestinal stem cells controls organ size and plasticity. Nature, 530(7590), 344–348. https://doi.org/10.1038/nature16953
49. Hoxha, V., Lama, C., Chang, P. L., Saurabh, S., Patel, N., Olate, N., & Dauwalder, B. (2013). Sex-specific signaling in the blood-brain barrier is required for male courtship in Drosophila. PLoS genetics, 9(1), e1003217. https://doi.org/10.1371/journal.pgen.1003217
50. Rubinstein, C. D., Rivlin, P. K., & Hoy, R. R. (2010). Genetic feminization of the thoracic nervous system disrupts courtship song in male Drosophila melanogaster. Journal of neurogenetics, 24(4), 234–245. https://doi.org/10.3109/01677063.2010.519805
51. Houot, B., Gigot, V., Robichon, A., & Ferveur, J. F. (2017). Free flight odor tracking in Drosophila: Effect of wing chemosensors, sex and pheromonal gene regulation. Scientific reports, 7, 40221. https://doi.org/10.1038/srep40221
52. Lu, B., Zelle, K. M., Seltzer, R., Hefetz, A., & Ben-Shahar, Y. (2014). Feminization of pheromone-sensing neurons affects mating decisions in Drosophila males. Biology open, 3(2), 152–160. https://doi.org/10.1242/bio.20147369
53. Baker, K. D., & Thummel, C. S. (2007). Diabetic larvae and obese flies-emerging studies of metabolism in Drosophila. *Cell metabolism*, *6*(4), 257–266. https://doi.org/10.1016/j.cmet.2007.09.002
54. Padmanabha, D., & Baker, K. D. (2014). Drosophila gains traction as a repurposed tool to investigate metabolism. *Trends in endocrinology and metabolism: TEM*, *25*(10), 518–527. https://doi.org/10.1016/j.tem.2014.03.011
55. Testa, N. D., Ghosh, S. M., & Shingleton, A. W. (2013). Sex-specific weight loss mediates sexual size dimorphism in Drosophila melanogaster. PloS one, 8(3), e58936.
56. Rideout, E. J., Narsaiya, M. S., & Grewal, S. S. (2015). The sex determination gene transformer regulates male-female differences in Drosophila body size. PLoS genetics, 11(12), e1005683.
57. De Groef, S., Ribeiro Lopes, M., Winant, M., Rosschaert, E., Wilms, T., Bolckmans, L., Calevro, F., & Callaerts, P. (2024). Reference genes to study the sex-biased expression of genes regulating Drosophila metabolism. Scientific reports, 14(1), 9518. https://doi.org/10.1038/s41598-024-58863-5
58. Millington, J. W., Brownrigg, G. P., Chao, C., Sun, Z., Basner-Collins, P. J., Wat, L. W., Hudry, B., Miguel-Aliaga, I., & Rideout, E. J. (2021). Female-biased upregulation of insulin pathway activity mediates the sex difference in Drosophila body size plasticity. eLife, 10, e58341. https://doi.org/10.7554/eLife.58341

59. Kurz, C. L., Charroux, B., Chaduli, D., Viallat-Lieutaud, A., & Royet, J. (2017). Peptidoglycan sensing by octopaminergic neurons modulates *Drosophila*oviposition. *eLife*, *6*, e21937. https://doi.org/10.7554/eLife.21937
60. Ramirez-Corona, B. A., Love, A. C., Chandrasekaran, S., Prescher, J. A., & Wunderlich, Z. (2022). Longitudinal monitoring of individual infection progression in drosophila melanogaster. *iScience*, *25*(11), 105378. https://doi.org/10.1016/j.isci.2022.105378
61. Masuzzo, A., Manière, G., Viallat-Lieutaud, A., Avazeri, É., Zugasti, O., Grosjean, Y., Kurz, C. L., & Royet, J. (2019). Peptidoglycan-dependent NF-κB activation in a small subset of brain octopaminergic neurons controls female oviposition. *eLife*, *8*, e50559. https://doi.org/10.7554/eLife.50559
62. Shahrestani, P., Chambers, M., Vandenberg, J., Garcia, K., Malaret, G., Chowdhury, P., Estrella, Y., Zhu, M., & Lazzaro, B. P. (2018). Sexual dimorphism in Drosophila melanogaster survival of Beauveria bassiana infection depends on core immune signaling. Scientific reports, 8(1), 12501. https://doi.org/10.1038/s41598-018-30527-1
63. Taylor, K., & Kimbrell, D. A. (2007). Host immune response and differential survival of the sexes in Drosophila. Fly, 1(4), 197–204. https://doi.org/10.4161/fly.5082
64. Millington, J. W., & Rideout, E. J. (2018). Sex differences in drosophila development and physiology. *Current Opinion in Physiology*, *6*, 46–56. https://doi.org/10.1016/j.cophys.2018.04.002
65. Ramond, E., Meister, M., & Lemaitre, B. (2015). From embryo to adult: Hematopoiesis along the drosophila life cycle. *Developmental Cell*, *33*(4), 367–368. https://doi.org/10.1016/j.devcel.2015.05.002
66. Brandt, S. M., & Schneider, D. S. (2007). Bacterial infection of fly ovaries reduces egg production and induces local hemocyte activation. *Developmental & Comparative Immunology*, *31*(11), 1121–1130. https://doi.org/10.1016/j.dci.2007.02.003
67. Abrams, J. (2005). Faculty opinions recommendation of aging of the innate immune response in drosophila melanogaster. *Faculty Opinions – Post-Publication Peer Review of the Biomedical Literature*. https://doi.org/10.3410/f.1024826.292872
68. Khadilkar, R. J., Vogl, W., Goodwin, K., & Tanentzapf, G. (2017). Modulation of occluding junctions alters the hematopoietic niche to trigger immune activation. *eLife*, *6*. https://doi.org/10.7554/elife.28081